IN THE UNITED STATES PATENT AND TRADEMARK OFFICE

In re Application of:

Ingham et al.

Serial No: 08/954,771

Filed: June 5, 1995

For: Vertebrate Tissue Pattern Inducing Proteins and Uses Related Thereto

Art Unit: 1646

Attorney Docket No. HMSU-P04-006

Examiner: M. Brannock

Assistant Commissioner for Patents
Washington, DC 20231

Declaration Under 35 U.S.C. §1.132 of Hank Dudek

Sir:

I, Hank Dudek of Massachusetts, hereby declare as follows:

1. I am an employee of Curis Inc., which licenses the above-described application from Harvard Medical School, the assignee of record.

2. Experiments were performed in collaboration with me, the results of which are depicted in Exhibits A-F, which demonstrate the effects of treating adult tissues with *sonic hedgehog* or *desert hedgehog*. Exhibit A shows that both *sonic hedgehog* and *desert hedgehog* induce expression of *gli-1* in endoneurial fibroblasts isolated from adult rat sciatic nerve. Exhibits B and C show that both *sonic hedgehog* and *desert hedgehog* improve recovery in adult mice following sciatic nerve crush. Exhibit D shows that striatal administration of *sonic hedgehog* induces *gli-1* in adult rats. Exhibits E and F show that *sonic hedgehog* attenuates malonate-induced lesions in adult rat. Each of these experiments demonstrates that *hedgehog* treatment affects adult tissues.

3. The above experiments were performed in accord with the teachings of the abovementioned patent application.

4. I hereby declare that all statements made herein of my own knowledge are true and that all statements made on information and belief are believed to be true; and further that these statements are made with knowledge that willful false statements and the like so made are

EXHIBIT 1

punishable by fine or imprisonment, or both, under Section 1001 of Title XVIII of the United States Code and that willful false statements may jeopardize the validity of this Application for Patent or any patent issuing thereon.

Hank Dudek

Dated: 12/13/01

Signature: Hank Dudek
Hank Dudek

EXHIBIT A

Dhh and Shh Induce *gli-1* expression in Endoneurial Fibroblasts Isolated From Adult Rat Sciatic Nerve

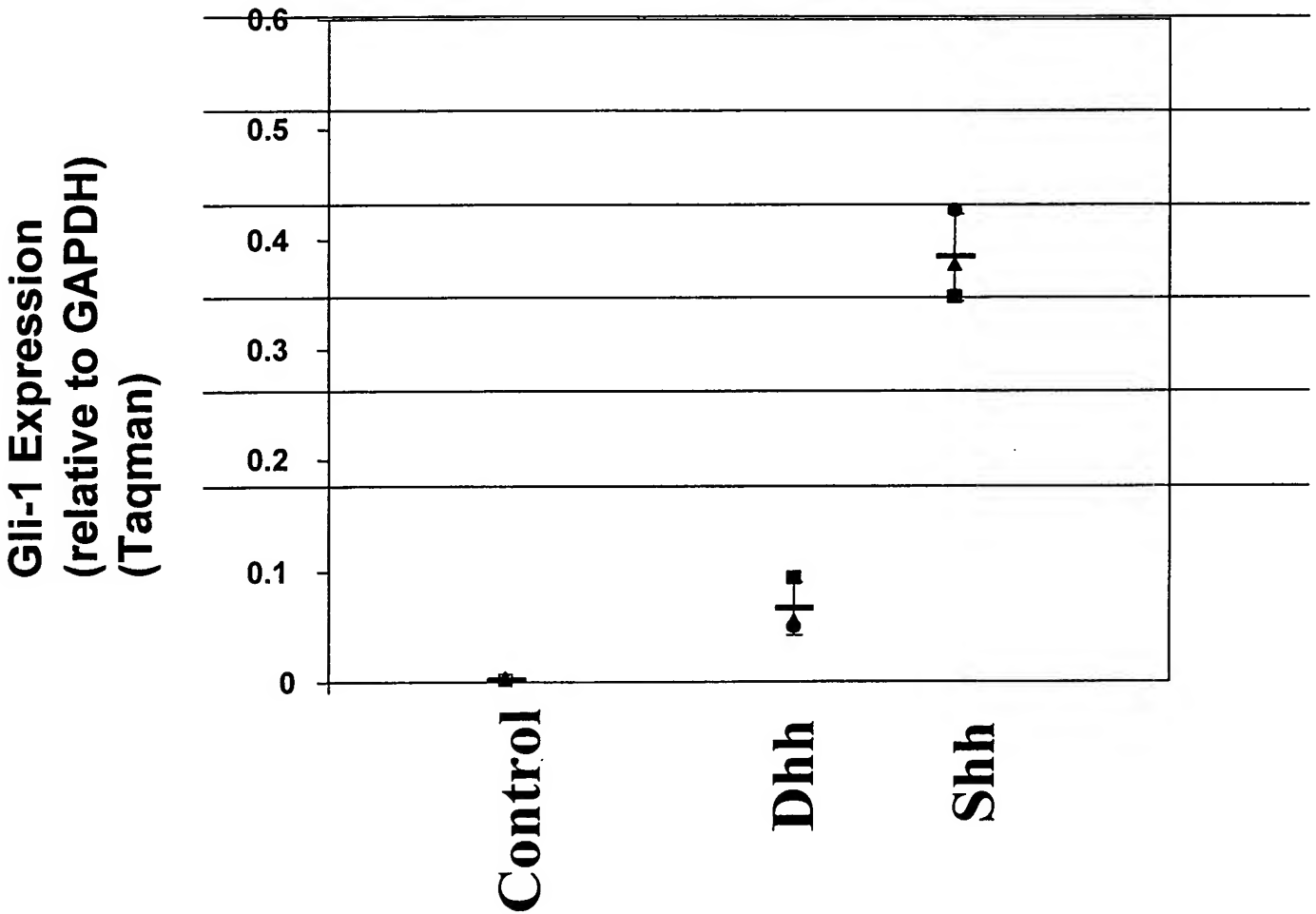

Shh and Dhh Improve Recovery After Sciatic Nerve Crush in Adult Mice

EXHIBIT B

Ability to Grip

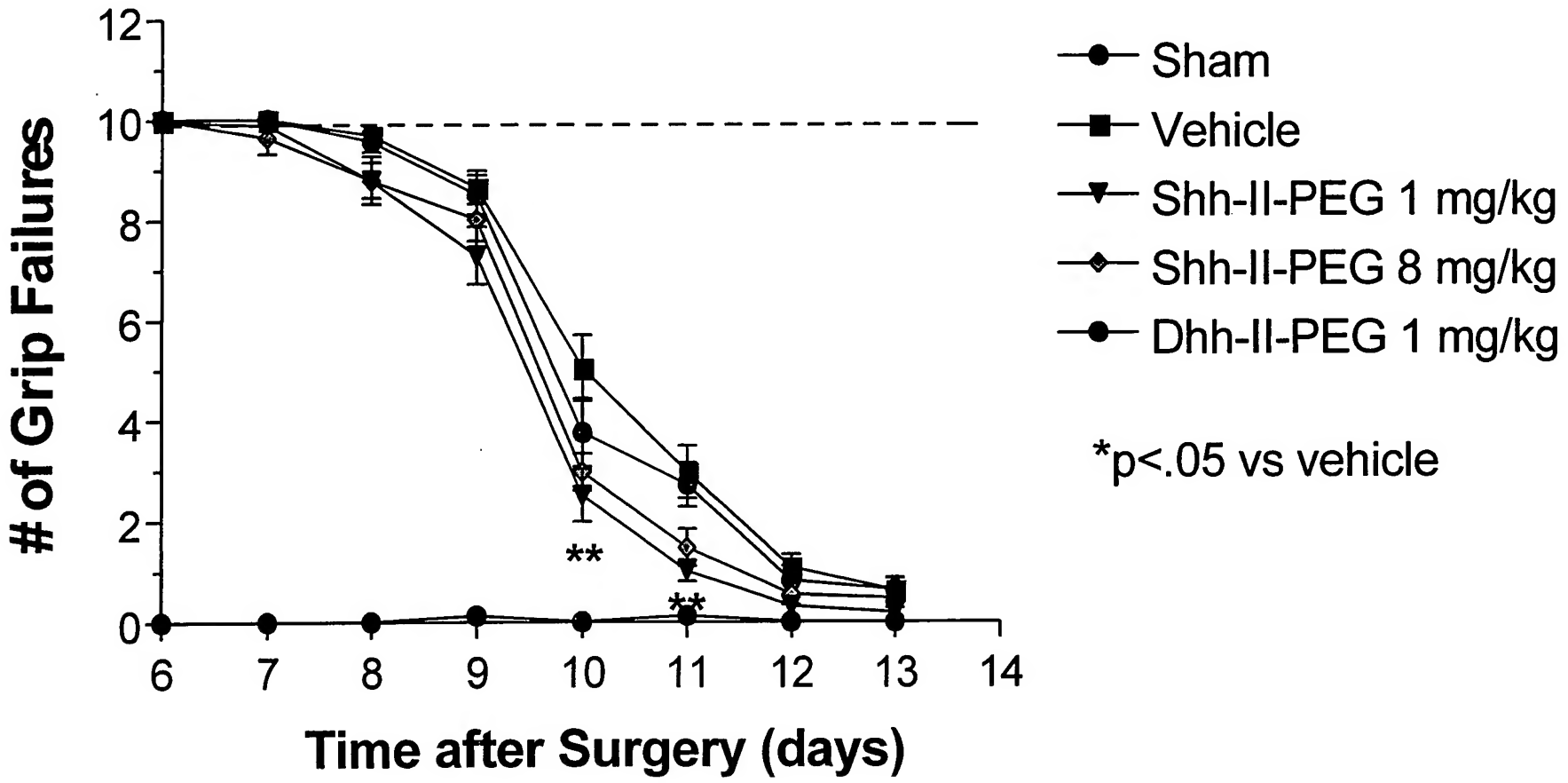

Shh Improves Recovery After Sciatic Nerve Crush in Adult Mice

EXHIBIT C

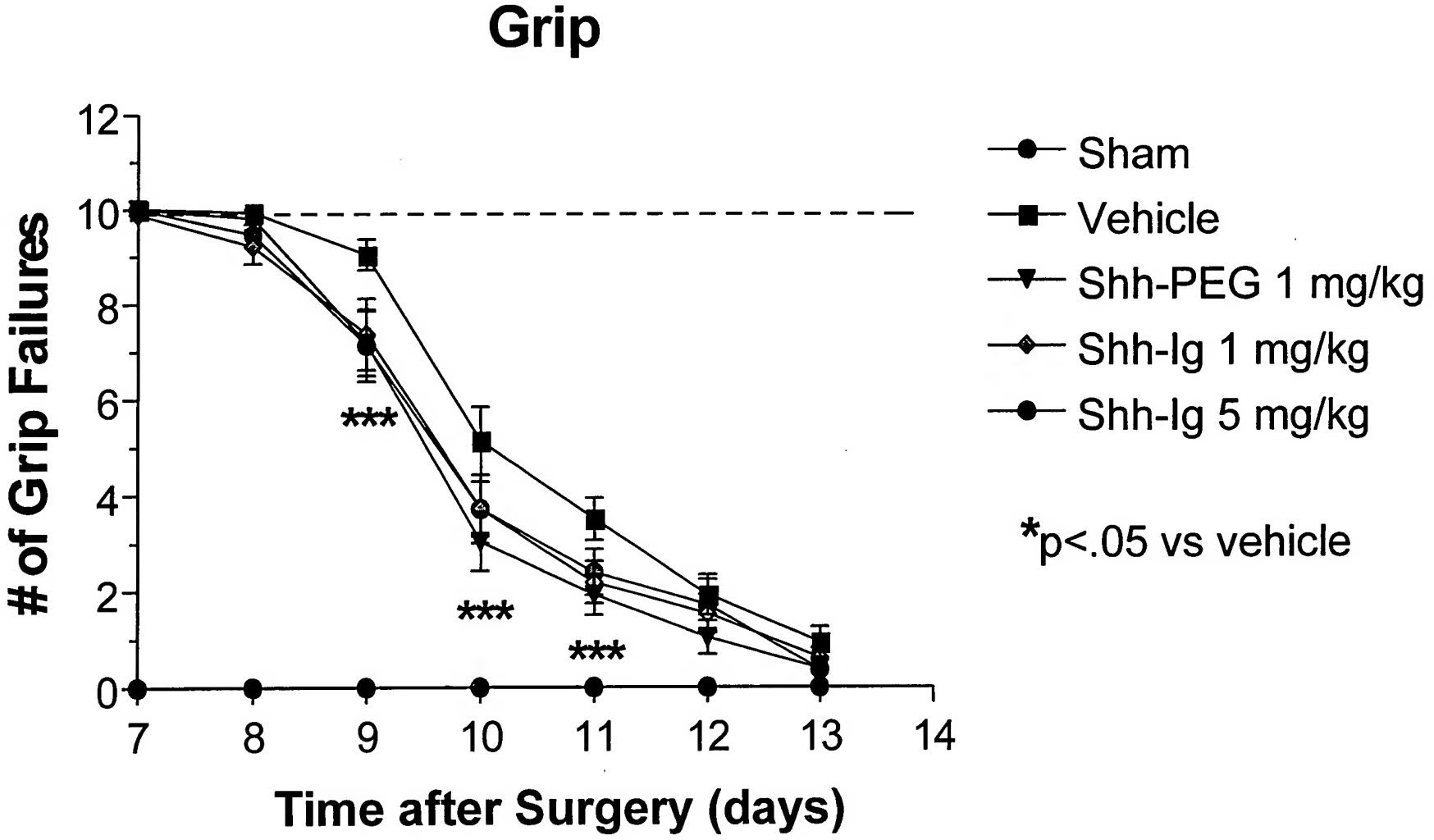

EXHIBIT D

Striatal Administration of Shh Induces *gli-1* in Adult Rats

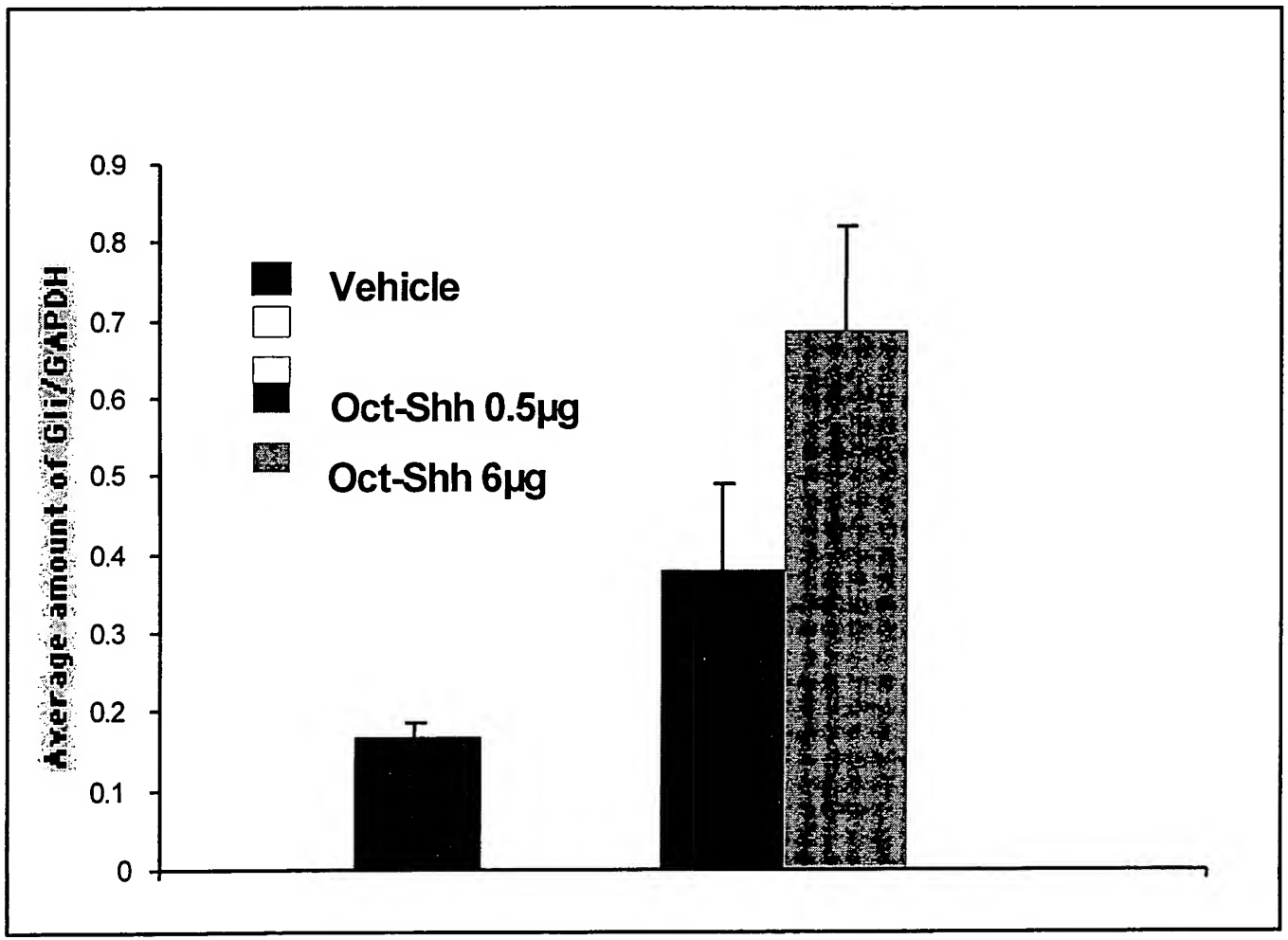

Striatal Administration of II-Shh Attenuates Malonate-Induced Lesion in Adult Rats

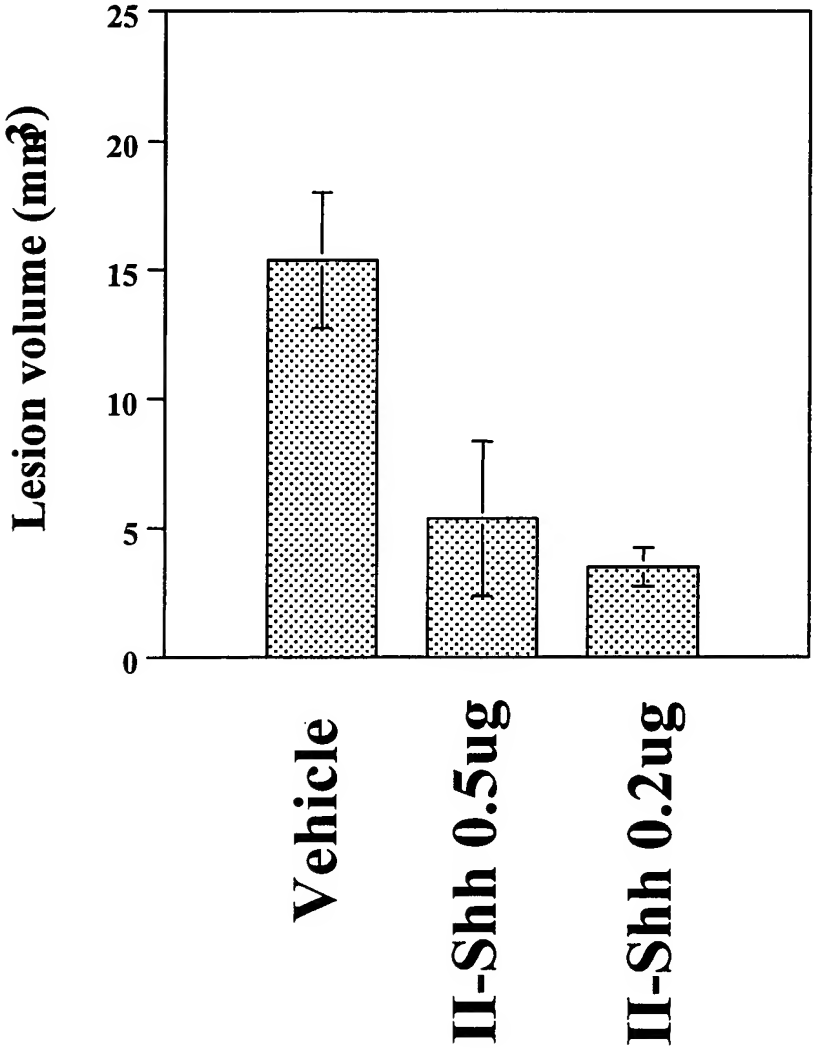

EXHIBIT E

Striatal Administration of Shh Attenuates Malonate-Induced Lesion in Adult Rats

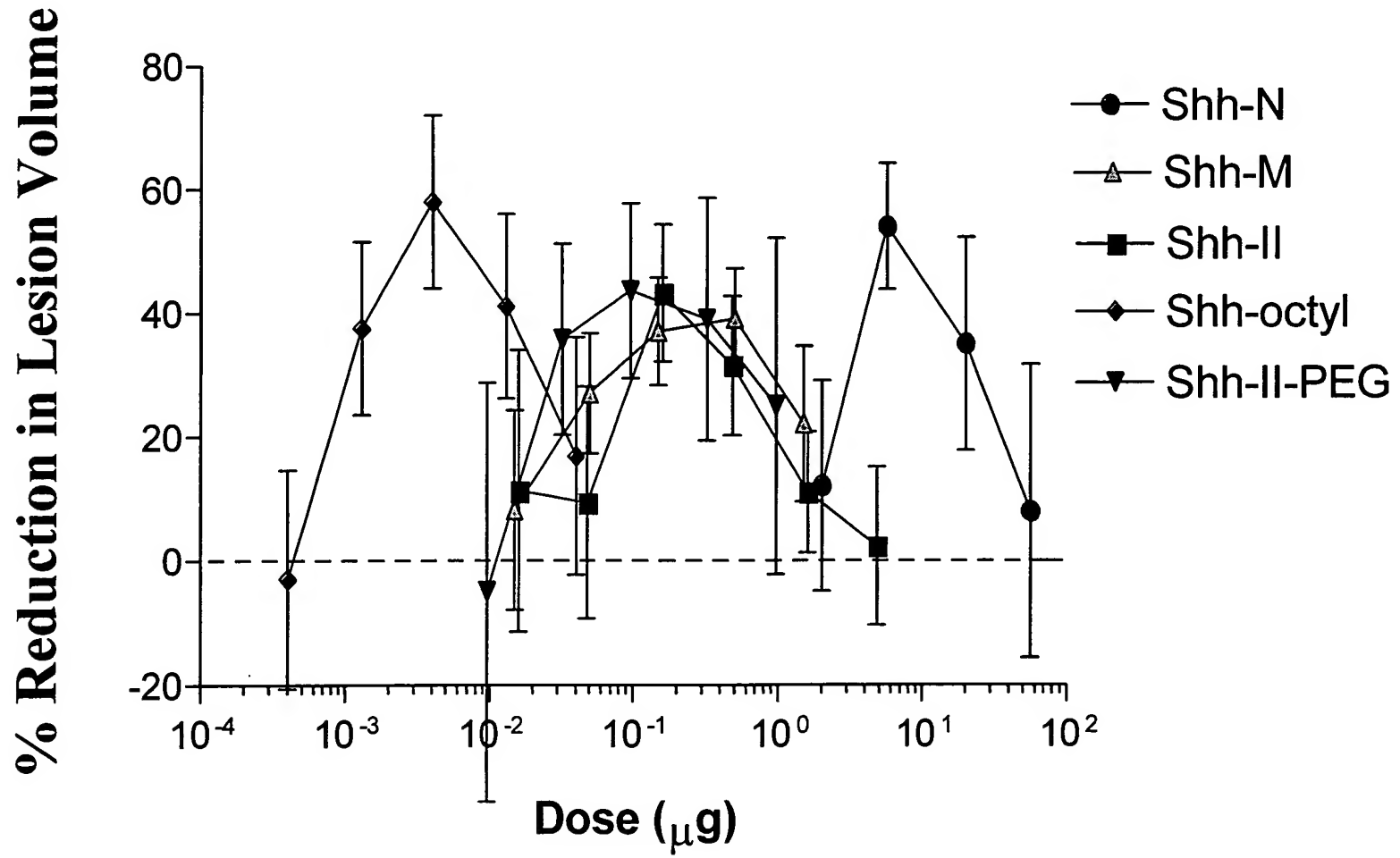

EXHIBIT F

The morphogen Sonic hedgehog is an indirect angiogenic agent upregulating two families of angiogenic growth factors

ROBERTO POLA[1], LEONA E. LING[2], MARCY SILVER[1], MICHAEL J. CORBLEY[2], MARIANNE KEARNEY[1], R. BLAKE PEPINSKY[2], RENEE SHAPIRO[2], FREDERICK R. TAYLOR[2], DARREN P. BAKER[2], TAKAYUKI ASAHARA[1] & JEFFREY M. ISNER[1]

[1]*Department of Medicine, St. Elizabeth's Medical Center, Tufts University School of Medicine, Boston, Massachusetts, USA*
[2]*Biogen Incorporated, Cambridge, Massachusetts, USA*
R.P. and L.E.L. contributed equally to this study.
Correspondence should be addressed to J.M.I.; email: vejeff@aol.com

Sonic hedgehog (Shh) is a prototypical morphogen known to regulate epithelial/mesenchymal interactions during embryonic development. We found that the hedgehog-signaling pathway is present in adult cardiovascular tissues and can be activated *in vivo*. Shh was able to induce robust angiogenesis, characterized by distinct large-diameter vessels. Shh also augmented blood-flow recovery and limb salvage following operatively induced hind-limb ischemia in aged mice. *In vitro*, Shh had no effect on endothelial-cell migration or proliferation; instead, it induced expression of two families of angiogenic cytokines, including all three vascular endothelial growth factor-1 isoforms and angiopoietins-1 and -2 from interstitial mesenchymal cells. These findings reveal a novel role for Shh as an indirect angiogenic factor regulating expression of multiple angiogenic cytokines and indicate that Shh might have potential therapeutic use for ischemic disorders.

Hedgehog (Hh) proteins act as morphogens in many tissues during embryonic development[1-8]. The mature forms of Hh are 19-kD proteins that interact with heparin through an N-terminal basic domain and are tethered to the cell membrane through cholesterol and fatty acyl modification[9-11]. Hh acts upon mesoderm in epithelial–mesenchymal interactions that are crucial to the formation of limb, lung, gut, hair follicles and bone[2-6]. Among the three highly conserved mammalian Hh genes, Sonic hedgehog (Shh) is the most widely expressed during development[12,13] and Shh deficiency in mice is embryonically lethal leading to multiple defects beginning in early to mid gestation[1,3-5]. Indian hedgehog (Ihh) is less widely expressed and Ihh-deficient mice survive to late gestation with skeletal and gut defects[4,6,13]. Desert hedgehog (Dhh) is expressed in the peripheral nerves, male gonads, as well as the endothelium of large vessels during development[13]. Dhh-deficient mice are viable but have peripheral-nerve and male-fertility defects[7,8].

Hh signaling occurs through the interaction of Hh protein with its receptor, Patched-1 (Ptc1 encoded by *Ptch*)[14]. This leads to activation of a transcription factor, Gli, which induces expression of downstream target genes including *Ptch* and *Gli* themselves[15-23]. Thus Ptc1 and Gli are both required components as well as transcriptionally induced targets of the Hh signaling pathway.

Several recent observations point to the involvement of Hh in vascularizing certain embryonic tissues. First, hypervascularization of neuroectoderm is seen following transgenic overexpression of Shh in the dorsal neural tube[24]. Second, Shh-deficient zebrafish exhibits disorganization of endothelial precursors and an inability to form the dorsal aorta or axial vein[25]. Third, Shh-deficient mice lack proper vascularization of the developing lung[3]. Fourth, Ihh, expressed by prehypertrophic chondrocytes, regulates the rate of chondrocyte maturation, a process closely correlated to the induction of angiogenesis in bone[26,27]. Finally, the induction of anagen in the hair follicle requires both Shh and angiogenesis[28,29]. Although these findings implicate the Hh pathway in vascular development, it is not clear whether these effects are due to a direct angiogenic action of Hh.

Here, we used postnatal mouse models to directly test the impact of Shh on vascularization *in vivo*. We show that cells in the adult cardiac and vascular tissues express Ptc1 and can respond to exogenous Hh by Ptc1 overexpression. In addition, we tested the angiogenic properties of Shh in the corneal and ischemic hind-limb models of angiogenesis. We found that Shh is a potent angiogenic factor, and when administered to aged mice it is able to induce robust neovascularization of ischemic hind-limbs. Shh-induced angiogenesis is characterized by large-diameter vessels. Investigation of the mechanism responsible for these findings established that Shh is an indirect angiogenic agent, inducing upregulation of two families of angiogenic growth factors, including vascular endothelial growth factor (VEGF) and the angiopoietins Ang-1 and Ang-2. Our data indicate a novel and unexpected biological activity for Hh with potential therapeutic implications.

Hh signaling in postnatal vasculature

In juvenile and adult mice, we found that Ptc1 is normally expressed in cardiovascular tissues (Fig. 1). We visualized Ptc1 expression using β-galactosidase (β-gal) staining of vascular tissues from mice that have a non-disruptive insertion of a nuclear localization signal (NLS)-tagged *lacZ* reporter gene upstream of the *Ptch* coding region (NLS-*Ptch-lacZ* mice). Ptc1 expression corresponds to *lacZ* expression in postnatal tissues and does not appear to be altered by *lacZ* insertion (L. Ling, unpublished observations). When examined for nuclear β-gal expression, NLS-*Ptch-lacZ* mice exhibited basal Ptc1 expression in adventitial cells,

EXHIBIT 2

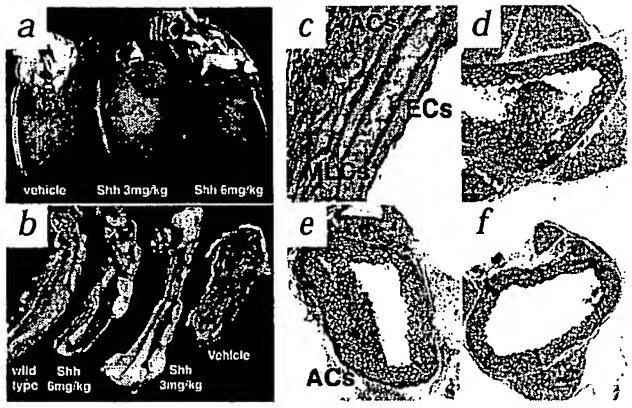

Fig. 1 *Ptch* expression and activation in postnatal cardiovascular tissues. ***a*** and ***b***, Hearts (*a*) and aortas (*b*) from NLS-*Ptch-lacZ*. Vehicle-treated mice exhibit a basal level of *Ptch* expression; administration of Shh result in a dose-dependent increase in *Ptch* expression in both hearts and aortas. ***c*** and ***d***, Paraffin cross sections from vehicle-treated mice (*c*) or untreated (*d*) mice show *Ptch* expression in endothelial cells (ECs), medial layer cells (MLCs) and adventitial cells (ACs). ***e*** and ***f***, Treatment with Shh (*e*) increases *Ptch* expression in adventitial cells. Aortas from wild-type littermates treated with Shh show no *Ptch* expression (*f* and *b*). Magnification ***c***, x200; ***d-f***, x100.

endothelial cells and cells in the medial layer of the vasculature (Fig. 1*c*). These results indicated that adult cardiovascular tissues have several resident populations of cells that might be responsive to Hh. To test this hypothesis, day 6 postnatal NLS-*Ptch-lacZ* mice were injected subcutaneously with Shh once daily for three days. This treatment induced a dose-dependent increase in Ptc1 expression in coronary arteries and aortas (Fig. 1*a*, *b* and *e*). In particular, adventitial cells showed a significant increase in Ptc1 expression (Fig. 1*e*). These cells were vimentin-positive, consistent with aortic adventitial fibroblasts (data not shown).

Shh induces vascular growth and promotes limb salvage

We tested the potential for Shh to act upon the adult vasculature and protect against ischemic injury by administering Shh, the VEGF-1 isoform recombinant human (rh)$VEGF_{165}$ or control to aged mice undergoing unilateral, surgically induced hind-limb ischemia. Aged mice have impaired angiogenesis, decreased blood-flow recovery, and typically develop limb necrosis from ischemic injury due to an inherent compromise in endogenous neovascularization[30]. A blinded evaluation showed that two-year-old mice receiving control developed profound consequences of hind-limb ischemia (including auto-amputation and foot/leg necrosis): 65% at day 7 after surgery, 73% at day 14, 80% at day 21, and 82% at day 28 (Fig. 2*a*). Similarly, mice treated with intramuscular injections of $rhVEGF_{165}$ had severe necrosis or auto-amputation of the ischemic limb comparable to vehicle-treated mice (data not shown). In contrast, we observed a sharp increase in limb salvage in mice treated with Shh. In this group, the percentage of auto-amputated limbs and foot/leg necrosis decreased to 25% at day 7 after surgery, 47% at day 14, 50% at day 21, and 50% at day 28 (Fig. 2*a*). Complete limb salvage after 21 and 28 days follow-up was obtained in half of the mice treated with Shh compared with less than 20% in the vehicle and $rhVEGF_{165}$-treated groups.

Laser power doppler imaging (LDPI) performed independently by two blinded operators demonstrated a progressive increase in the blood flow of ischemic hind limbs in Shh-treated mice, with significant differences seen at day 28 ($P < 0.01$) (Fig. 2*b*). In contrast, we observed no significant increase in hind-limb perfusion beyond 28 days of follow-up in control mice. At day 28 after surgery, the Doppler flow ratio was significantly increased in Shh-treated mice in comparison to the groups treated with $rhVEGF_{165}$ or vehicle ($P < 0.05$) (Fig. 2*b* and data not shown).

Likewise, capillary density at day 28 after surgery was significantly increased in Shh-treated versus $rhVEGF_{165}$- and control-treated mice ($P < 0.001$ and $P < 0.0001$, respectively) (Fig. 2*c*, *d* and data not shown). Neovascularization induced by Shh was characterized not only by increased numbers of capillaries, but also by a substantial increase in vessel diameter (Fig. 2*d*).

Shh-induced angiogenesis has distinctive morphology

To determine the basis of augmented neovascularization in response to Shh, we used the murine corneal angiogenesis model. We implanted pellets containing Shh and/or VEGF, or control in the corneas of 8–12-week-old C57BL/6J mice. Six days after implantation, both VEGF- and Shh-treated eyes exhibited growth of neovessels whereas none induced by control pellets (Fig. 3*a*, *b* and *c*). Whole-mount fluorescent BS1 lectin (Bandeiraea simplicifolia lectin-1, an endothelial cell marker) staining and CD31 immunostaining of cross sections showed several striking differences in morphology between Shh-induced neovessels and those induced by VEGF. Consistent with the previous observations in the is-

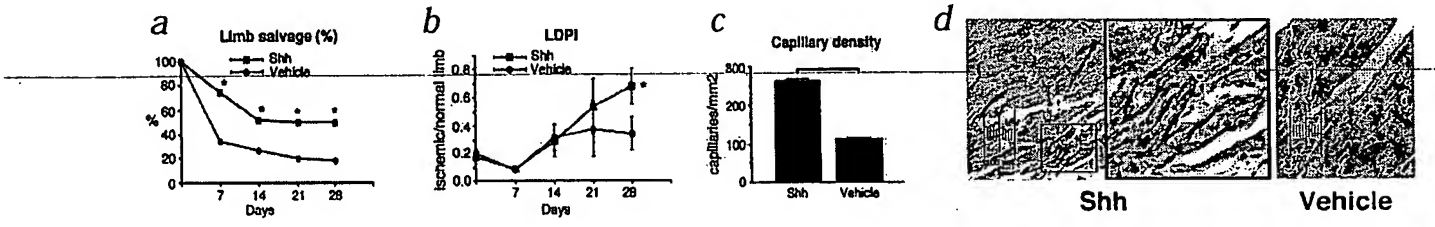

Fig. 2 Shh increases limb salvage, blood flow and capillary density in the setting of ischemia. ***a***, Limb salvage: at each time point, the percentage of limb salvage is statistically significantly higher in Shh-treated group (■) compared with vehicle (●). *, $P < 0.05$. ***b***, Blood flow: ischemic/normal leg perfusion ratio is extremely low in both groups immediately after surgery, but progressively increases over time in Shh-treated mice (■), achieving significant improvement by day 28. *, $P < 0.01$. In contrast, no increase in hind-limb perfusion was seen over time in mice treated with vehicle (●). Ischemic/normal leg perfusion ratio at day 28 is significantly higher in Shh-treated mice compared with vehicle (0.681 ± 0.126 versus 0.344 ± 0.119; $P < 0.05$). ***c***, Capillary density at day 28 after surgery is significantly increased in mice treated with Shh compared with vehicle ($P < 0.0001$). ***d***, Representative pictures of capillary density show that the number of vessels is increased in Shh-treated tissues. A higher magnification (x400) of Shh-treated skeletal muscle (middle) shows a substantial increase in vessel diameter.

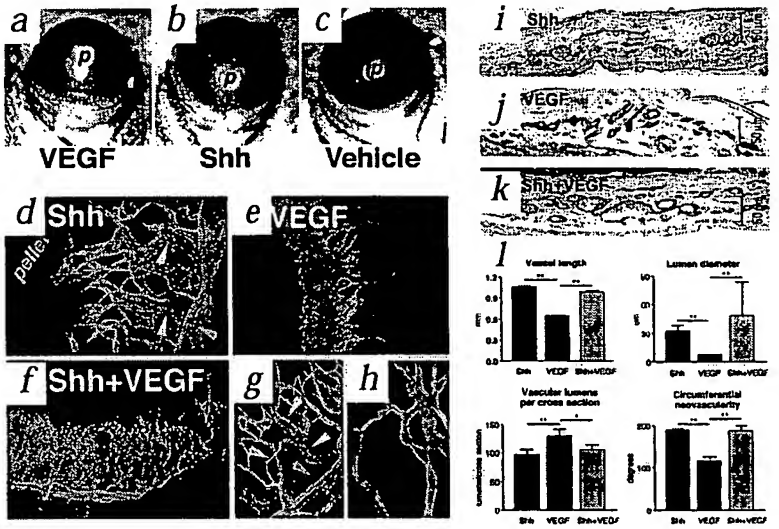

Fig. 3 Shh-induced angiogenesis has unusual morphological characteristics. ***a–e***, Neovascular growth is detectable in corneas implanted with pellets ('p') containing VEGF (*a*) and Shh (*b*), but not vehicle (*c*). ***d–h***, Shh (*d*, *g* and *h*), VEGF (*e*) and Shh+VEGF (*f*) induce vessels with different morphology. Red arrowheads indicate the main limbus artery, blue arrowheads indicate the main limbus vein, white arrowheads indicate expanded venous structures and the yellow arrowhead indicates an arteriovenous shunt. *h* shows branching vessels induced by Shh. ***i–k***, 5-μm cross sections of corneas treated with Shh (*i*), VEGF (*j*) or Shh+VEGF (*k*), immunostained for CD-31 (brown) show differences in vessel diameters induced by each treatment. ***l***, Vessel length, circumferential extent of neovascularity and average lumen diameter are significantly higher in Shh-treated corneas. When added to VEGF, Shh is able to increase average vascular lumen diameter (upper right); the large s.e.m. in Shh+VEGF-treated corneas reflects the presence of capillaries and large-diameter vessels. The number of vascular lumens per cross section is higher in VEGF-treated group. **, $P < 0.0001$; *, $P < 0.001$.

chemic hind-limb model, Shh-induced neovasculature consisted of large, branching vessels that grew directly from the limbus vessels and often extended to and surrounded the pellet at the apex of the new vessel growth (Fig. 3*b*, *d*, *g*, *h* and *i*). Many of these vessels exhibited dichotomous branching, creating a complex and well-organized vascular tree (Fig. 3*h*). The average number of branching vessels in corneal neovascularization induced by Shh was 7.3 ± 1.4 per field (data not shown). In contrast, VEGF implantation resulted in capillaries of lesser lumenal caliber that were uniformly distributed along the cornea (Fig. 3a, *e* and *j*). Shh-induced neovasculature also exhibited numerous large-diameter vessels that did not arise as branches of the limbus artery, but appeared to be venous structures that often formed arteriovenous shunts (Fig. 3*d* and *g*). The average length of Shh-induced neovessels was significantly greater than that of vessels induced by VEGF (1.05 ± 0.18 versus 0.67 ± 0.09 mm; $P < 0.0001$) (Fig. 3*l*). The circumferential extent of Shh-induced neovasculature was also increased compared with VEGF (190 ± 3.9 versus 116 ± 9.6 degrees; $P < 0.0001$) (Fig. 3*l*). Histological evaluation demonstrated increased lumenal diameters in Shh-induced versus VEGF-induced neovessels (32.62 ± 5.82 versus 7.25 ± 0.7 μm; $P < 0.0001$) (Fig. 3*i*, *j* and *l*). In both the Shh and VEGF groups, the number of perienthelial cells was limited with no significant difference (3.52 ± 1.66 versus 4.88 ± 1.75 smooth muscle cells per cross section, respectively; P = NS) (data not shown). In addition, the combination of Shh and VEGF showed lengthened, large-diameter neovessels like those seen with Shh alone, but also exhibited characteristics of VEGF-induced vasculature, that is, a dense area of fine vessels close to the implanted pellet (Fig. 3*f* and *k*). Thus, Shh and VEGF together appeared to produce an intermediate phenotype containing a variety of neovascular lengths and diameters (Fig. 3*f*, *k* and *l*).

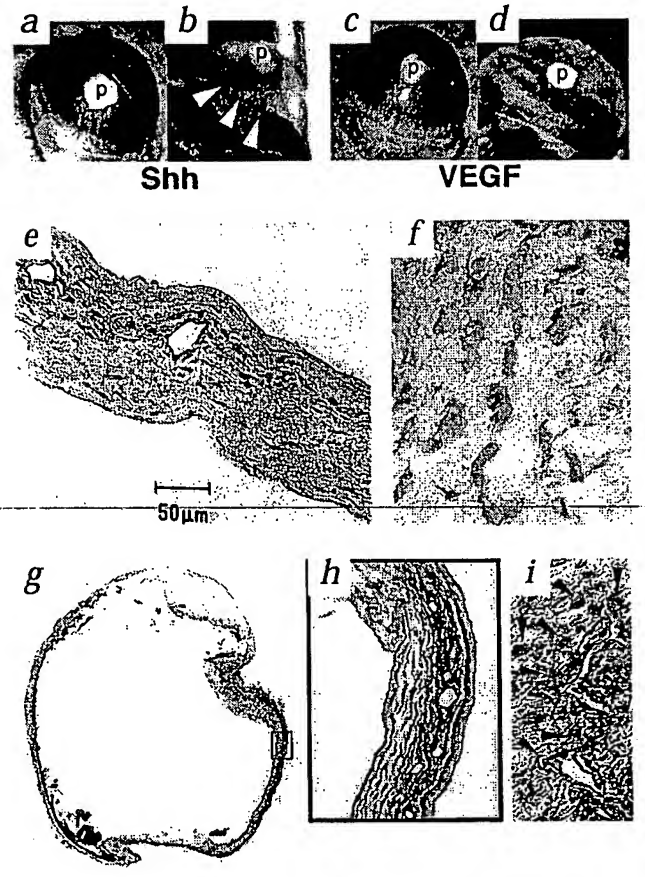

Ptc1 mediates Shh-induced angiogenesis in fibroblasts

To determine the identity of cells directly activated by Shh during corneal angiogenesis, we implanted pellets containing Shh

Fig. 4 Shh acts upon stromal cells and induces VEGF production. ***a–d***, Macroscopic photographs of corneal neovascularization induced by pellets ('p') containing Shh (*a*) and VEGF (*c*) and correspondent β-gal staining for Ptc1 in Shh-treated (*b*) and VEGF-treated (*d*) corneas. β-gal–positive staining is detectable in correspondence of Shh-induced angiogenesis (arrowheads in *b*), but not of VEGF-induced angiogenesis (*d*). ***e–i***, Cross sections of Shh-treated corneas, prepared as in *b*, immunostained for CD-31 (*e*), vimentin (*f*) or VEGF at magnifications of ×20 (*g*), ×100 (*h*) and ×400 (*i*). VEGF staining is localized only in the neovascular area (*g*), around the neovessels (*h* and *i*). Cells with β-gal–positive nuclei have VEGF-positive cytoplasm (red arrowheads in *i*).

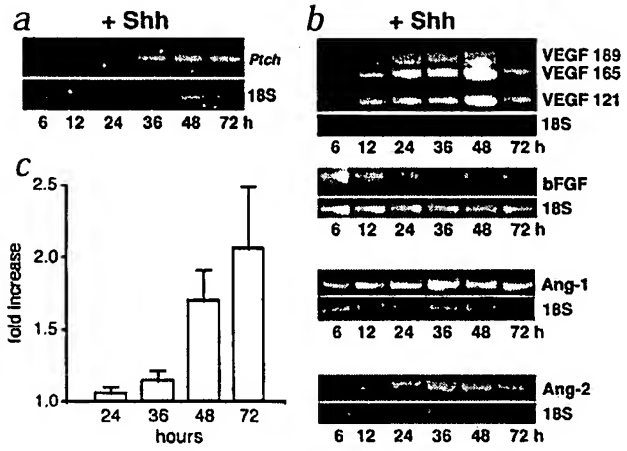

Fig. 5 Shh upregulates *Ptch*, VEGF and angiopoietins in human fibroblasts. ***a*** and ***b***, Quantitative RT-PCR for *Ptch* (*a*) and angiogenic cytokines (*b*) shows that fibroblasts respond to Shh by upregulating Ptc1, all 3 isoforms of VEGF-1, Ang-1 and -2, while bFGF is downregulated. ***c***, Conditioned media from Shh-stimulated compared with vehicle-stimulated human lung fibroblasts shows a ~2-fold increase in $VEGF_{165}$ (mean ± s.e.m.) detected by ELISA between 48 and 72 h in this representative experiment.

or VEGF into the cornea of NLS-*Ptch-lacZ* mice. After collecting them, we stained corneas for β-gal to detect Ptc1 expression. Strong β-gal staining was detected around the neovascular foci of NLS-*Ptch-lacZ* eyes treated with Shh, indicating that Shh activates the Hh pathway during neovascularization (Fig. 4*a* and *b*). In contrast, VEGF-treated corneas were β-gal-negative, indicating that VEGF does not induce expression of Ptc1 (Fig. 4*c* and *d*). Histological analysis showed that β-gal-positive cells were not endothelial cells (CD31-negative) or periendothelial cells (α-smooth-muscle-actin-negative, data not shown), but were consistent with interstitial fibroblasts (vimentin-positive) surrounding the neovessels (Fig. 4*e* and *f*). The β-gal-positive cells as well as their surrounding matrix were also immunopositive for VEGF, indicating that Shh might stimulate—either directly or indirectly—VEGF expression within the neovascular foci (Fig. 4*g*, *h* and *i*).

Shh upregulates *Ptch* and induces VEGF and Ang-1 and -2

We tested the possibility that Shh might induce fibroblasts to produce angiogenic cytokines by treating fibroblasts in culture with Shh protein and evaluating the induction of *Ptch*, VEGF and other angiogenic cytokines. Quantitative reverse transcriptase (RT)-PCR showed that a number of primary fibroblasts and fibroblast cell lines responded to Shh stimulation by upregulating *Ptch* (Fig. 5*a* and data not shown). Comparison of *Ptch* expression in Shh-treated and vehicle-treated fibroblasts at various time points showed that *Ptch* was induced within 6–12 hours after addition of Shh to the medium, and continued to increase up to 72 hours. In contrast, the absence of *Ptch* upregulation by endothelial cells in the corneal neovessels was mirrored *in vitro* by the inability of human umbilical vein endothelial cells (HUVECs) or microvascular endothelial cells to respond to Shh by *Ptch* upregulation, proliferation, migration or serum-free survival (data not shown).

In addition to upregulating *Ptch*, Shh stimulated cultured fibroblasts to increase expression of angiogenic growth factors, including all three isoforms of VEGF-1 and both Ang-1 and Ang-2 (Fig. 5*b*). Upregulation of mRNA encoding $VEGF_{121}$, $VEGF_{165}$ and $VEGF_{189}$ was first detected at 12 hours and continued to increase up to 48 hours in Shh-stimulated compared with vehicle-stimulated cells at each time point. This increase in VEGF-1 mRNA correlated with a significant increase in $VEGF_{165}$ protein (Fig. 5*c*). Finally, Shh treatment also upregulated Ang-1 and Ang-2 mRNA (Fig. 5*b*). In contrast, expression of bFGF was decreased after Shh treatment (Fig. 5*b*). These results demonstrate that Shh induces a specific subset of angiogenic growth factors including the VEGF-1 isoforms as well as Ang-1 and Ang-2.

Discussion

Our results clearly show that Shh has angiogenic activity. Shh induces robust neovascularization in the setting of ischemia and may have important therapeutic utility in the treatment of ischemic disorders. Neovascularization induced by Shh appears to be mediated by stromal cells producing a combination of potent angiogenic factors, including VEGF, Ang-1 and Ang-2. *In vitro*, most fibroblasts cell lines respond to Shh by *Ptch* upregulation (Fig. 5*a* and data not shown). However, repeated attempts to activate HUVECs, aortic and microvascular endothelial cells by Shh treatment were unsuccessful. These cells show no proliferation, serum-free survival, migration or upregulation of Ptc1 in response to Shh proteins (data not shown). Ptc1 was not upregulated on endothelial cells in Shh-treated corneas or in endothelial cells of aortas from Shh-treated mice. Despite this, endothelial cells do express Ptc1 *in vitro* and *in vivo* and the possibility that Shh affects endothelial cells cannot therefore be completely excluded.

Our data instead indicate that neovascularization induced by Shh might be triggered through Shh/Ptc1 signaling specifically in mesenchymal cells. Fibroblasts are a well-known source of VEGF during development, tumor growth, hypoxia and inflammation[31–34]. Our data raise the possibility that VEGF production from fibroblasts might be mediated by the Hh pathway. Similar indirect mechanisms of inducing angiogenesis have been demonstrated for PDGF (platelet-derived growth factor) BB and TGF (tumor growth factor) β1 , both of which promote angiogenesis via upregulation of VEGF and basic fibroblast growth factor (bFGF)[35]. Given this precedent, we propose that Shh acts upon interstitial mesenchymal cells (such as fibroblasts in the cornea) to induce an array of angiogenic growth factors, including three isoforms of VEGF-1 as well as Ang-1 and Ang-2. The ability to upregulate these angiogenic cytokines in concert appears thus far unique to Shh. There are no previous reports of Ang-1 expression being regulated by other cytokines, morphogens, growth factors or ischemia.

Here we show that the angiogenic response to Shh is characterized by long, tortuous vessels with large diameters. It has been shown that vessels with increased length, diameter and branching are induced when Ang-1 acts synergistically with VEGF (ref. 36). We show here that Shh upregulates both VEGF and Ang-1; however, Shh induces an even more complex vascular system. When Shh is used, the quantitative and qualitative features of the vessels are more pronounced and they are also associated with vascular tortuosity. The basis for this remains to be elucidated, but it is possible that exogenous administration of VEGF and Ang-1 together might not be comparable to localized activation of these growth factors in stromal cells by Shh. Localized overexpression of VEGF and Ang-1 in the skin of transgenic mice, for example, produces

similar large-diameter, long and distinctly branching vessels[37]. Moreover, the sequence and magnitude of upregulation of these cytokines by Shh *in vivo* is unknown. Shh also upregulates Ang-2 and all three isoforms of VEGF-1. In colon cancer, compared with tumors expressing only one or two VEGF-1 isoforms, the coordinated expression of three VEGF-1 isoforms correlates with more aggressive tumors, as shown by vein invasion and metastasis leading to a poor prognosis[38]. The particular combination of angiogenic growth factors induced by Shh might thus contribute to the robust and distinct character of its neovascularization.

VEGF has been implicated in the earliest stage of vasculogenesis, during endothelial-cell differentiation and plexus formation, but also in postnatal angiogenesis through its ability to induce endothelial-cell migration and proliferation[39]. Ang-1 is required for both embryonic remodeling of the vascular plexus and postnatal vessel remodeling involving sprouting, branching or vessel maturation[39]. *In vivo* studies reveal that Ang-1 acts in a complementary and coordinated fashion with VEGF, mediating interactions between endothelial cells and surrounding support cells[40]. Ang-2 acts as a natural antagonist of Ang-1 (ref. 40). Whereas Ang-1 is expressed widely in normal adult tissues, Ang-2, in its role in continuous vascular stabilization, is highly expressed only at sites of vascular remodeling in order to allow the vessels to revert to a more plastic and unstable state[40]. Ang-2 is expressed along with VEGF in tumor vasculature and the two together might function as an angiogenic signal at the growing periphery of tumors[40]. Our study indicates that Shh upregulates both Ang-1 and Ang-2. The significance and relevance of this concomitant activation is unclear. We suggest that in the case of Shh-induced angiogenesis, VEGF might initiate the angiogenic response and angiopoietins could subsequently antagonize each other in a complex process of recruitment, stabilization and remodeling of neovasculature.

Shh-induced vessels tend to bifurcate into two branches that eventually split again. Previous reports show that tracheal splitting and branching during lung organogenesis are regulated by the Hh/Ptc1/Gli pathway through a number of effects including FGF inhibition[3]. We observed evidence of bFGF dowregulation in fibroblasts treated with Shh, and that the Shh-induced vessels are highly branched. The vascular network induced by Shh is also characterized by several venous structures with arterovenous shunts. This vasculature is functional, as demonstrated by the increase in perfusion and consequent rate of limb salvage in aged mice with limb ischemia. These experiments indicate that Shh might have therapeutic uses in promoting angiogenesis in the ischemic disorders.

The signaling pathway by which Hh upregulates these angiogenic growth factors remains to be determined. *Ptch* and many other Hh-inducible genes are regulated by the Hh pathway transcriptional factor Gli. However, no Gli response elements are present in the VEGF or Ang-1 promoter regions. Hh can, however, also induce a Gli-independent pathway that activates the orphan nuclear receptor, COUPTFII (ref. 41). Interestingly, COUPTFII-deficient embryos are defective in maturation of the primary vascular plexus and exhibit decreased Ang-1 expression[42]. Thus it is possible that Hh induces at least Ang-1 via COUPTFII activation in mesenchymal cells.

The development of functional vasculature requires precise spatial-temporal regulation of cell proliferation, migration, interaction and differentiation. The role of Shh as a morphogen might be relevant to its potential activity to orchestrate appropriate spatial-temporal production of angiogenic growth factors during embryonic and postnatal angiogenesis, which in addition must be coordinated with muscle, bone and nerve development. This report thus establishes novel biological and potentially therapeutic activities for Shh. The discovery of angiogenic activity for Shh, combined with its known morphogenic functions in development, indicates that Shh might coordinate epithelial/stromal interactions with the ingrowth of vasculature during development. Given that Shh can promote limb salvage in aged mice through the enhancement of blood flow and capillary density and induction of large caliber vessel formation, we suggest that Shh merits investigation as proangiogenic therapy for ischemic disorders.

Methods

Mice. Male C57BL/6J mice (Jackson Labs, Bar Harbor, Maine), heterozygous male or female NLS-*Ptch-lacZ* mice or their wild-type littermates (Ontogeny, Cambridge, Massachusetts) were used. All experiments were conducted in accordance with St. Elizabeth's or Biogen Institutional Animal Care and Use Committee.

Systemic treatment with Shh. Postnatal day 6 NLS-*Ptch-lacZ* mice were treated with daily subcutaneous injections of 10–20 µL of polyethylene glycol 20,000-conjugated C24II/A192C Shh N-terminal protein or vehicle[43]. Hearts and aortas were collected at postnatal day 9 and stained for β-gal expression.

Ischemic hind-limb model. Unilateral hind-limb ischemia was created in 2-year-old C57BL/6J mice[44]. Eighty mice were operated and treated with intramuscular injections of 1 mg/kg Shh–mIgG1 fusion protein, vehicle or 100 µg/kg of rhVEGF$_{165}$ (Chemicon, Temecula, California). Injections were once every other day during the first week, once every 3 days during the second week, and twice during the third and fourth weeks. At predetermined time points, necrosis and hind-limb perfusion were examined by two blinded operators[44]. Mice were then killed for histological analysis. Hind limbs were fixed in 100% methanol and cut in paraffin sections. Capillaries were counted by two blinded observers[44]. Shh–mIgG1 has increased half-life and activity *in vivo* (Shapiro *et al.*, manuscript in preparation). It contains residues Cys24–Gly197 of the human Shh coding sequence with two mutations: Cys24Ilelle and KRRH(32–35)QRRP, with a 16-fold increased activity *in vitro* compared with unmodified mature human Shh protein produced *E. Coli* (Taylor *et al.*, manuscript in preparation). The Fc region of mouse IgG1 was fused directly downstream of Gly127. The glycosylation site was destroyed with a Gln to Asn mutation. Protein was expressed in *Pichia pastoris* GS115 (Invitrogen, Carlsbad, California) using a pPIC9-derived vector and the α-mating-factor secretion signal. The protein was purified and sequenced as described[10,45].

Cornea neovascularization assay. Pellets containing one of the following were implanted in C57BL76J mice[36]: 1.5 µg myristoylated-Shh protein (Myr-Shh), 0.3 µg VEGF (R&D Systems, Minneapolis, Minnesota), 1.5 µg Myr-Shh + 0.3 µg VEGF, or vehicle. In NLS-*Ptch-lacZ* mice pellets contained Myr-Shh 1.5 µg/pellet, VEGF 0.3 µg/pellet or vehicle. Myr-Shh was prepared by chemical myristoylation (Taylor *et al.*, manuscript in preparation) of the α-amino group of Cys24 (of *E. Coli*-produced mature human Shh protein) followed by repurification and sequencing[10,45]. Myr-Shh exhibited 160-fold increased activity *in vitro* compared with mature human Shh protein (Cys24–Gly197).

Histology. Tissues from NLS-*Ptch-lacZ* mice were fixed in 0.2% gluteraldehyde, washed, stained overnight at 37 °C in 1 mg/mL X-gal, 5 mM potassium ferricyanide, 5 mM potassium ferrocyanide, 2 mM $MgCl_2$, 0.01% sodium deoxycholate, 0.02% Nonidet P-40, 50 mM Na_2HPO_4 pH8, and visualized as whole mounts or paraffin sections. For immunohistochemistry, eyes were fixed in 100% methanol or in 1% paraformaldehyde. Corneal hemispheres were cut into paraffin or frozen sections. Endothelial cells were identified using rat monoclonal antibody against mouse CD31 (Pharmingen, San Diego, California) and a biotinylated goat

immunoglobulin against rat. For periendothelial cells, a mouse monoclonal antibody against smooth muscle α-actin conjugated with alkaline-phosphatase (Sigma,) was used. For VEGF, a rabbit polyclonal antibody against VEGF (Santa Cruz Biotechnology, Santa Cruz, California) and a biotinylated goat immunoglobulin antibody against rabbit (Signet Labs, Dedham, Massachusetts) were used. Staining for vimentin was done with goat serum against vimentin (Sigma) compared with normal goat serum (Sigma) using horseradish peroxidase-conjugated donkey secondary antibody against goat (Jackson Immunoresearch, West Grove, Pennsylvania). For fluorescence microscopy, mice received an intravenous bolus of 500 μg of FITC-conjugated BS-1 lectin (Vector, Burlingame, California) 30 min before death. Eyes were fixed in 1% paraformaldehyde, and the dissected corneas were placed on glass slides.

Competitive RT-PCR. RNA was extracted from CCD37 human lung fibroblasts (ATCC) stimulated *in vitro* with MyrShh or vehicle. cDNA was obtained and amplified using the SuperScript preamplification system (Gibco-BRL, Paisley, UK). Signals were normalized to 18S rRNA using optimal 18S primer/Competimer ratios as determined for each target gene following the manufacturer's recommendations (Ambion, Austin, Texas) or to GAPDH, using GAPDH control reagents and Taqman analysis (PE Applied Biosystems, Foster City, California). The following primer pairs and PCR conditions were used. Ptc1: 5′-TCAGGATGCATTTGACAGTGACTGG-3′ and 5′- ACTCCGAGTCGGAGGAATCAGACCC-3′ with 25 cycles of 94 °C (30 s), 55 °C (1 min) and 72 °C (1 min). VEGF: 5′-CGAAGTGGTGAAGTTCATGGATG-3′ and 5′-TTCTGTATCAGTCTTTCCTGGTGAG-3′ with 30 cycles of 94 °C (30 s), 62 °C (1 min) and 72 °C (1 min). bFGF: 5′-TACAACTTCAAGCAGAAGAG-3′ and 5′-CAGCTCTTAGCAGACATTGG-3′ with 25 cycles of 94 °C (30 s), 62 °C (1 min), and 72 °C (1 min). Ang-1: 5′-CAACACAAACGCTCTGCAGAGAGA-3′ and 5′-CTCCAGTTGCTGCTTCTGAAGGAC-3′ with 25 cycles of 94 °C (30 s) and 64 °C (90 s). Ang-2: 5′-AGCGACGTGAGGATGGCAGCGTT-3′ and 5′-ATTTCCTGGTTGGCTGATGCTGCTT-3′ with 32 cycles of 94 °C (30 s) and 64 °C (90 s).

ELISA. $VEGF_{165}$ in conditioned media from MyrShh-stimulated cells were compared with vehicle-stimulated cells. $VEGF_{165}$ was measured per manufacturer's instructions using the Quantikine human VEGF-ELISA kit (R&D Systems, Minneapolis, Minnesota). All experiments were performed in triplicate.

Statistical analysis. All results are expressed as mean ± s.e.m. Differences were analyzed by ANOVA or χ-square test and considered statistically significant at $P < 0.05$.

Acknowledgments

We thank K. Strauch and E. Garber for the design and generation of recombinant Shh-mIgG1 fusion protein and J. Mead, E. Barban and T. Aprahamian for technical assistance.

RECEIVED 24 JANUARY; ACCEPTED 30 APRIL 2001

1. Chiang, C. *et al.* Cyclopia and defective axial patterning in mice lacking sonic hedgehog gene function. *Nature* **383**, 407–413 (1996).
2. Johnson, R.L. & Tabin, C.J. Molecular models for vertebrate limb development. *Cell* **90**, 979–990 (1997).
3. Pepicelli, C.V., Lewis, P.M. & McMahon, A.P. Sonic hedgehog regulates branching morphogenesis in the mammalian lung. *Curr. Biol.* **8**, 1083–1086 (1998).
4. Ramalho-Santos, M., Melton, D.A. & McMahon, A.P. Hedgehog signals regulate multiple aspects of gastrointestinal development. *Development* **127**, 2763–2772 (2000).
5. St-Jacques, B. *et al.* Sonic hedgehog signaling is essential for hair development. *Curr. Biol.* **8**, 1058–1068 (1998).
6. St-Jacques, B., Hammerschmidt, M. & McMahon, A.P. Indian hedgehog signaling regulates proliferation and differentiation of chondrocytes and is essential for bone formation. *Genes Dev.* **13**, 2072–2086 (1999).
7. Bitgood, M.J., Shen, L. & McMahon, A.P. Sertoli cell signaling by Desert hedgehog regulates the male germline. *Curr. Biol.* **6**, 298–304 (1996).
8. Parmantier, E. *et al.* Schwann cell-derived Desert hedgehog controls the development of peripheral nerve sheaths. *Neuron* **23**, 713–724 (1999).
9. Porter, J.A., Young, K.E. & Beachy, P.A. Cholesterol modification of hedgehog signaling proteins in animal development. *Science* **274**, 255–259 (1996).
10. Pepinsky, R.B. *et al.* Identification of a palmitic acid-modified form of human Sonic hedgehog. *J. Biol. Chem.* **273**, 14037–14045 (1998).
11. Fuse, N. *et al.* Sonic hedgehog signals not as a hydrolytic enzyme but as an apparent ligand for patched. *Proc. Natl. Acad. Sci. USA* **96**, 10992–10999 (1999).
12. Zardoya, R., Abouheif, E. & Meyer, A. Evolution and orthology of hedgehog genes. *Trends Genet.* **12**, 496–497 (1996).
13. Bitgood, M.J. & McMahon, A.P. Hedgehog and Bmp genes are coexpressed at many diverse sites of cell–cell interaction in the mouse embryo. *Dev. Biol.* **172**, 126–138 (1995).
14. Ingham, P.W. Transducing hedgehog: the story so far. *EMBO J.* **17**, 3505–3511 (1998).
15. Stone, D.M. *et al.* Characterization of the human suppressor of fused, a negative regulator of the zinc-finger transcription factor Gli. *J. Cell. Sci.* **112**, 4437–4448 (1999).
16. Kogerman, P. *et al.* Mammalian Suppressor-of-Fused modulates nuclear-cytoplasmic shuttling of Gli-1. *Nature Cell. Biol.* **1**, 312–319 (1999).
17. Ding, Q. *et al.* Mouse suppressor of fused is a negative regulator of sonic hedgehog signaling and alters the subcellular distribution of Gli. *Curr. Biol.* **9**, 1119–1122 (1999).
18. Monnier, V., Dussillol, F., Alves, G., Lamour-Isnard, C. & Plessis, A. Suppressor of fused links fused and Cubitus interruptus on the hedgehog signaling pathway. *Curr. Biol.* **8**, 583–586 (1998).
19. Sisson, J.C., Ho, K.S., Suyama, K. & Scott, M.P. Costal2, a novel kinesin-related protein in the Hedgehog signaling pathway. *Cell* **90**, 235–245 (1997).
20. Robbins, D.J. *et al.* Hedgehog elicits signal transduction by means of a large complex containing the kinesis-related protein costal2. *Cell* **90**, 225–234 (1997).
21. Kalderon, D. Hedgehog signalling: Ci complex cuts and clasps. *Curr. Biol.* **7**, R759–R762 (1997).
22. Marigo, V., Johnson, R.L., Vortkamp, A. & Tabin, C. Sonic hedgehog differentially regulates expression of GLI and GLI3 during limb development. *Dev. Biol.* **180**, 273–283 (1996).
23. Marigo, V. & Tabin, C. Regulation of patched by sonic hedgehog in the developing neural tube. *Proc. Natl. Acad. Sci. USA* **93**, 9346–9351 (1996).
24. Rowitch, D. H. *et al.* Sonic hedgehog regulates proliferation and inhibits differentiation of CNS precursor cells. *J. Neurosci.* **19**, 8954–8965 (1999).
25. Brown, L.A. *et al.* Insights in to early vasculogenesis revealed by expression of the ETS-domain transcription factor Fli-1 in type and mutant zebrafish embryos. *Mech. Dev.* **90**, 237–252 (2000).
26. Vu, T. H. *et al.* MMP-9/gelatinase B is a key regulator of growth plate angiogenesis and apoptosis of hypertrophic chondrocytes. *Cell* **93**, 411–422 (1998).
27. Zhou, Z. *et al.* Impaired endochondral ossification and angiogenesis in mice deficient in membrane-type matrix metalloproteinase I *Proc. Natl. Acad. Sci. USA* **97**, 4052–4057 (2000).
28. Mecklenburg, L. *et al.* Active hair growth (anagen) is associated with angiogenesis. *J. Invest. Dermatol.* **114**, 909–916 (2000).
29. Wang, L.C. *et al.* Conditional disruption of hedgehog signaling pathway defines its critical role in hair development and regeneration. *J. Invest. Dermatol.* **114**, 901–908 (2000).
30. Rivard, A. *et al.* Age-dependent impairment of angiogenesis. *Circulation* **99**, 111–120 (1999).
31. Scheid, A. *et al.* Hypoxia-regulated gene expression in fetal wound regeneration and adult wound repair. *Pediatr. Surg. Int.* **16**, 232–236 (2000).
32. Volpert, O.V., Dameron, K.M. & Bouck, N. Sequential development of an angiogenic phenotype by human fibroblasts progressing to tumorigenicity. *Oncogene* **14**, 1492–1502 (1997).
33. Detmar, M. *et al.* Hypoxia regulates the expression of vascular permeability factor/vascular endothelial growth factor (VPF/VEGF) and its receptor in human skin. *J. Invest. Dermatol.* **108**, 263–268 (1997).
34. Cho, C.S. *et al.* CD40 engagement on synovial fibroblasts up-regulates production of vascular endothelial growth factor. *J. Immunol.* **164**, 5055–5061 (2000).
35. Brogi, E. *et al.* Indirect angiogenesis cytokines upregulate VEGF and bFGF gene expression in vascular smooth muscle cells, while hypoxia upregulates VEGF expression only. *Circulation* **90**, 649–652 (1994).
36. Asahara, T. *et al.* Tie2 receptor ligands, angiopoietin-1 and angiopoietin-2, modulate VEGF-induced postnatal neovascularization. *Circ. Res.* **83**, 233–240 (1998).
37. Suri, C. *et al.* Increased vascularization in mice overexpressing angiopoietin-1. *Science* **282**, 468–471 (1998).
38. Tokunaga, T. *et al.* Vascular endothelial growth factor (VEGF) mRNA isoforms expression pattern is correlated with liver metastasis and poor prognosis in colon cancer. *Br. J. Cancer* **77**, 998–1002 (1998).
39. Gale, N.W. & Yancopoulos, G.D. Growth factors acting via endothelail cell-specific receptor tyrosine kinases: VEGFs, angiopoietins, and ephrins in vascular development. *Genes Dev.* **13**, 1055–1066 (1999).
40. Holash, J. *et al.* New model of tumor angiogenesis: dynamic balance between vessel regression and growth mediated by anglopoietins and VEGF. *Oncogene* **18**, 5356–5362 (1999).
41. Krishnan, V. *et al.* Mediation of Sonic hedgehog-induced expression of COUP-TFII by a protein phosphatase. *Science* **278**, 1947–1950 (1997).
42. Pereira, F.A. *et al.* The orphan nuclear receptor COUP-TFII is required for angiogenesis and heart development. *Genes Dev.* **13**, 1037–1049 (1999).
43. Pepinsky, R.B. *et al.* Mapping sonic hedgehog-receptor interactions by steric interference. *J. Biol. Chem.* **275**, 10995–11001 (2000).
44. Couffinhal, T. *et al.* A mouse model of angiogenesis. *Am. J. Pathol.* **152**, 1667–1679 (1998).
45. Williams, K.P. *et al.* Functional antagonists of sonic hedgehog reveal the importance of the N terminus for activity. *J. Cell. Sci.* **112**, 4405–4414 (1999).

Hedgehog Signaling Regulation of Insulin Production By Pancreatic β-Cells

Melissa K. Thomas, Naina Rastalsky, Jee H. Lee, and Joel F. Habener

Hedgehogs (Hhs) are intercellular signaling molecules that regulate tissue patterning in mammalian development. Mammalian Hhs include Sonic hedgehog (Shh), Indian hedgehog (Ihh), and Desert hedgehog (Dhh). The absence of Shh expression is required for the early development of the endocrine and exocrine pancreas, but whether Hh signaling functions in the fully developed adult endocrine pancreas is unknown. Here we report that Hhs Ihh and Dhh and their receptors patched (Ptc) and smoothened are expressed in the endocrine islets of Langerhans of the fully developed rat pancreas and in the clonal β-cell line INS-1. We demonstrate the coexpression of Ptc with insulin in β-cells of mouse pancreatic islets, indicating that β-cells are targets of active Hh signaling. The administration of cyclopamine, a Hh signaling inhibitor, decreases both insulin secretion from and insulin content of INS-1 cells. The effects of Hh signaling on insulin production occur at the transcriptional level because activation of Hh signal transduction by ectopic expression of Shh increases rat insulin I promoter activation in a dose-dependent manner in transient transfections of INS-1 and MIN6 β-cell lines. In contrast, inhibition of Hh signaling with increasing concentrations of cyclopamine progressively reduces insulin promoter activity. Furthermore, the treatment of INS-1 cells with cyclopamine diminishes endogenous insulin mRNA expression. We propose that Hh signaling is not restricted to patterning in early pancreas development but also continues to signal in differentiated β-cells of the endocrine pancreas in regulating insulin production. Thus, defective Hh signaling in the pancreas should be considered as a potential factor in the pathogenesis of type 2 diabetes.
***Diabetes* 49:2039–2047, 2000**

The intercellular signaling molecules known as hedgehogs (Hhs) are critical regulators of development. Hh signaling regulates segment polarity (1–3), wing and limb growth, and patterning in *Drosophila* (4–8). Multiple vertebrate Hhs have been identified, including Sonic hedgehog (Shh), Indian hedgehog (Ihh), and Desert hedgehog (Dhh) (9). Shh mediates patterning of limbs, specification of cell types in the central nervous system, and organ development (10–12) and is implicated in the development of left-right asymmetry (13–16). Ihh regulates proliferation and differentiation of chondrocytes in skeletal morphogenesis and participates in the development of mammary glands (17–19). Dhh signaling is important for testicular Sertoli cell function and for the formation of peripheral nerve sheaths (20,21).

Vertebrate Hhs are processed in a manner analogous to their *Drosophila* homologue, Hh, internally cleaved by an autocatalytic process to produce NH_2- and COOH-terminal Hh products (22). Cholesterol is covalently attached to the NH_2-terminal domain of Hhs via cholesterol transferase activity located in the COOH-terminal domain (22), and this modification may regulate Hh sequestration and movement through cells (23–25). The secreted NH_2-terminal Hh fragments bind directly to the receptor patched (Ptc) (26). The binding of Hhs to Ptc results in release of the membrane-bound protein smoothened (Smo) from tonic inhibition. Activation of Smo leads to transcriptional activation of target genes, in some instances due to activation of transcription factors in the Gli (derived from glioblastoma)/Cubitus interruptus (Ci) family of zinc finger DNA-binding proteins (27,28). The vertebrate Hh proteins Shh, Ihh, and Dhh interact with the identical Ptc and Smo receptor signaling systems, demonstrate similar biologic properties, and use the same Hh signal transduction pathway to activate target gene transcription (21,27,29,30).

The *ptc* gene is the best characterized transcriptional target of Hh signaling. The induction of the *ptc* gene by Hh signaling likely is mediated by Gli/Ci transcription factors that have binding sites within the Ptc promoter (31). Localized higher levels of Ptc expression indicate the presence of a transcriptionally active Hh signaling pathway in flies and mice (30,32,33).

During the early development of the pancreas in higher vertebrates, Shh is differentially expressed in the foregut. At embryonic day 10.5 in the mouse, the dorsal and ventral pancreatic endoderm from which the pancreas buds do not express Shh or Ihh, in contrast to the lateral gut endoderm in which Hhs are expressed. Ptc is expressed in the gastrointestinal mesoderm but not in the pancreatic mesenchyme (34). These patterns of Hh expression suggest that the absence of Shh expression permits mesodermal differentiation and pancreas development. Signals from the notochord permit the development of the dorsal pancreas in chick embryo pancreas explants (35). Repression of endodermal Shh expression in this system induces the expression of insulin and other

From the Laboratory of Molecular Endocrinology, Massachusetts General Hospital, Howard Hughes Medical Institute, Harvard Medical School, Boston, Massachusetts.

Address correspondence and reprint requests to Joel F. Habener, MD, Laboratory of Molecular Endocrinology, Massachusetts General Hospital, 55 Fruit St., WEL320, Boston, MA 02114. E-mail: jhabener@partners.org.

Received for publication 20 March 2000 and accepted in revised form 21 August 2000.

Ci, Cubitus interruptus; Dhh, Desert hedgehog; Gli, derived from glioblastoma; Hh, hedgehog; Ihh, Indian hedgehog; PDX-1, pancreas duodenum homeobox-1; PBS, phosphate-buffered saline; PCR, polymerase chain reaction; Ptc, patched; RT, reverse transcriptase; Shh, Sonic hedgehog; Smo, smoothened.

EXHIBIT 3

pancreas-specific genes (36). Local exposure of the foregut of embryonic chicks to cyclopamine, an inhibitor of Hh signaling (37), promotes heterotopic expression of cells producing the endocrine and exocrine pancreas proteins, insulin and carboxypeptidase A, respectively (38). Misexpression of Shh in the developing pancreatic endoderm in transgenic mice results in a dysmorphogenic pancreas surrounded by smooth muscle cells; endocrine pancreatic cells expressing the hormones insulin (β-cells) and glucagon (α-cells) develop, but the architecture of the endocrine pancreas consisting of the islets of Langerhans is markedly disorganized (34).

Although studies of early pancreas development suggest that the absence of Hh signaling is required, we asked whether Hh signaling may function in a different context in the fully developed endocrine pancreas. We find that Hhs and their receptors are expressed in pancreatic islets of the adult animal and that Hh signaling stimulates insulin gene expression in differentiated pancreatic β-cells. These findings raise the possibility that defective Hh signaling in the endocrine pancreas may contribute to the pathogenesis of type 2 diabetes.

RESEARCH DESIGN AND METHODS

Plasmid construction. The full-length cDNA for mouse Shh was provided by A. McMahon. The pShh plasmid was constructed by subcloning mouse Shh cDNA into a pED expression vector (39) obtained from C.P. Miller (Genetics Institute, Cambridge, MA). The plasmid –410INS-LUC consists of a fragment of the rat insulin I gene promoter that spans nucleotides –410 to 49 inserted into the pXP2 vector that includes firefly luciferase reporter sequences (40).

Cell culture. INS-1 cells, provided by C. Wollheim (41), were cultured in 11.1-mmol/l glucose in RPMI 1640 medium supplemented with 10% fetal bovine serum, 10 mmol/l HEPES buffer, 1 mmol/l sodium pyruvate, 100 U/ml penicillin G sodium, 100 μg/ml streptomycin sulfate, 0.25 μg/ml amphotericin B (Gibco Life Technologies, Gaithersburg, MD), and 71.5 μmol/l β-mercaptoethanol (Sigma, St. Louis, MO). MIN6 cells, provided by J. Miyazaki, were cultured in 25 mmol/l glucose as described (42). Cyclopamine (provided by W. Gaffield, U.S. Department of Agriculture) was prepared as a stock solution of 10 mmol/l in 95% ethanol and diluted in culture medium to the final concentration indicated. Cells were treated as specified with cyclopamine solutions or ethanol carrier (control) solutions.

Immunohistochemistry. For dual fluorescence immunocytochemistry, INS-1 cells were grown in slide culture chambers (Nunc, Naperville, IL). Mouse pancreas was embedded and frozen on dry ice in Tissue-Tek O.C.T. compound (Sakura Finetek, Torrance, CA). Tissue sections (7 μm) or cells were fixed for 5 min at 25°C in 4% paraformaldehyde in phosphate-buffered saline (PBS), washed with PBS, and blocked with 1% donkey serum followed by an overnight incubation at 4°C with the indicated primary antisera. Specimens were rinsed in PBS and incubated for 1 h with secondary antisera as indicated and mounted with mounting medium (Kirekegaard and Perry Laboratories, Gaithersburg, MD). Primary antisera included goat polyclonal IgG anti-Ihh COOH-terminus [Ihh (C-15)], goat polyclonal IgG anti-Dhh COOH-terminus [Dhh (M-20)], goat polyclonal IgG anti-Ptc [Patched (G-19)], goat polyclonal IgG anti-Smo [Smo (N-19)] (each at a 1:500 dilution; Santa Cruz Biotechnology, Santa Cruz, CA), and guinea pig polyclonal anti-insulin (1:300 dilution; Linco Research, St. Charles, MO). Preadsorption of goat polyclonal IgG anti-Ihh COOH-terminus antiserum [Ihh (C-15)] with blocking peptide was conducted according to the manufacturer's instructions (Santa Cruz Biotechnology). Donkey anti-goat IgG Cy3 (1:1,500 dilution) and donkey anti–guinea pig IgG Cy2 (1:500 dilution) (Jackson Immuno Research Laboratories, West Grove, PA) were used as secondary antisera. As a negative control, mouse pancreas sections were also prepared with guinea pig polyclonal anti-insulin antisera without primary goat polyclonal IgG, followed by incubation with donkey anti-goat IgG Cy3 and donkey anti–guinea pig IgG Cy2. No pancreatic islet Cy3 immunofluorescence was observed under these conditions. A Nikon Epifluorescence microscope equipped with an Optronics TEC-470 camera (Optronics Engineering, Goleta, CA) was used to capture images and interfaced with a Power Macintosh 7100 computer. Image processing and analyses were performed with IP Lab Spectrum (Signal Analytics, Vienna, VA) and Adobe Photoshop (Adobe Systems, San Jose, CA) software.

Transfections. INS-1 cells were transfected with 5–6 μg total DNA and 10 μl Lipofectamine according to the manufacturer's instructions (Gibco). Cells were harvested 24 h after transfection with 1× Reporter lysis buffer (Promega, Madison, WI). In selected studies, ~90 min before transfection, cells were pretreated with 0, 1, 10, or 20 μmol/l cyclopamine in 0.19% ethanol in serum-free medium; at the time of transfection, 0, 1, 10, or 20 μmol/l cyclopamine in 0.19% ethanol was added to the final transfection cocktail; and after 5 h of incubation with the transfection cocktail, cells were incubated in fresh INS-1 culture medium with 0, 1, 10, or 20 μmol/l cyclopamine in 0.19% ethanol for an additional 24 h before harvest. Luciferase assays were conducted in duplicate with the Luciferase Assay System, as outlined by the manufacturer (Promega). Luciferase activities were normalized to protein concentrations of the extracts as determined by the Bio-Rad Protein Assay (Bio-Rad, Hercules, CA). Fold-activation was determined by normalizing the luciferase units per microgram protein at each point within a transfection to the activity of the pED empty vector that was designated as 100%. Data are presented as means ± SE, with P values calculated by Student's t tests (Microsoft Excel Software; Microsoft, Redmond, WA).

Reverse transcriptase–polymerase chain reactions. Total RNA was isolated from cells and islets with Tri-Reagent (Sigma) using a modified guanidine thiocyanate and phenol extraction method outlined in the manufacturer's protocol. For preparation of cDNA, total cellular RNA was preincubated with 50 ng/μl oligo(dT)12-18 (Gibco) at 70°C for 10 min and immediately chilled on ice. The addition of 0.5 U/μl RNase Inhibitor (Cloned), 1× first-strand buffer, 0.01 mol/l dithiothreitol, 1 mmol/l dATP, 1 mmol/l dTTP, 1 mmol/l dCTP, and 1 mmol/l dGTP (Gibco) to the reaction was followed by a 2-min incubation at 42°C. The final reaction was conducted with the addition of (reverse transcriptase [RT]$^+$) Moloney murine leukemia virus RT (SuperScript II RT; Gibco) or (RT$^-$) RNase-free water with a 1-h incubation at 42°C followed by a 15-min incubation at 70°C.

For polymerase chain reaction (PCR) amplification, the following primers were used: for a 266-nucleotide fragment of Ptc cDNA spanning nucleotides 390–656 of mouse Ptc (GenBank acc. no. U46155), sense primer 5′-TCAGAA GATAGGAGAAGA-3′ and antisense primer 5′-TCCAAAGGTGTAATGATTA-3′ were used; for a 372-nucleotide fragment of Smo cDNA spanning nucleotides 386–758 of rat Smo (GenBank acc. no. U84402), sense primer 5′-TGCTGTGT GCTGTCTACAT-3′ and antisense primer 5′-AGGGTGAAGAGTGTACAGA-3′ were used; for a 387-nucleotide fragment of Ihh cDNA spanning nucleotides 22–409 of rat Ihh (GenBank acc. no. AF162914), sense primer 5′-AGGACCGT CTGAACTCAC-3′ and antisense primer 5′-TTGCCATCTTCCCCCATG-3′ were used; and for a 331-nucleotide fragment of Dhh spanning nucleotides 47–378 of rat Dhh (GenBank acc. no. AF148226), sense primer 5′-GTTACGTGCG CAAGCA-3′ and antisense primer 5′-GCCTTCGTAGTGCAGT-3′ were used. PCR amplifications were conducted with a PerkinElmer 9600 Thermocycler with Taq polymerase (TaKaRa, Takara Shuzo, Otsu, Japan).

Southern blots. PCR products were subjected to agarose gel electrophoresis and stained with ethidium bromide for visualization before transfer to nylon membranes (Magnacharge; Micron Separations, Westboro, MA). Membranes were probed with [^{32}P]-radiolabeled oligonucleotides as follows: nucleotides 529–564 of mouse Ptc cDNA (GenBank acc. no. U46155) with the sequence 5′-TACATGTATAACAGGCAATGGAAGTTGGAACATTTG-3′, nucleotides 621–644 of rat Smo cDNA (GenBank acc. no. U84402) with the sequence 5′-CAAGAG CTGGTACGAGGACGTGGA-3′, nucleotides 338–364 of rat Ihh cDNA (GenBank acc. no. AF162914) with the sequence 5′-AACTGGGGAGCGTGTGGCC CTGTCAGC-3′, and nucleotides 96–117 of rat Dhh cDNA (GenBank acc. no. AF148226) with the sequence 5′-TAGTATGCCCGAGCGGACCCTT-3′.

Insulin assays. Insulin levels were measured with a Rat Insulin RIA Kit (Linco Research) using the protocol outlined by the manufacturer. To determine insulin secretion rates, fresh culture medium, to which cyclopamine in 0.19% ethanol or 0.19% ethanol carrier was added as indicated, was applied to cultured INS-1 cells. After 24 h of incubation, 500-μl aliquots of culture medium were removed and serially diluted for the assay. Culture medium that was not exposed to cells was tested as a negative control for the assay. In some experiments, transfected cells were assessed for insulin secretion rates. In these experiments, after preincubation with cyclopamine in 0.19% ethanol or 0.19% ethanol carrier, lipofectamine, and DNA, the transfected cells received fresh culture medium with cyclopamine in 0.19% ethanol or 0.19% ethanol carrier, and 24-h insulin secretion rates were assessed.

To determine cellular insulin content, INS-1 cells were incubated for 24 h with fresh culture medium and cyclopamine in 0.19% ethanol or 0.19% ethanol carrier, as indicated. Cells were then rinsed in PBS and lysed in 0.1 N HCl in 100% ethanol at 4°C. The lysate was incubated overnight at –70°C. The thawed lysate was vortexed and subjected to brief centrifugation at 14,000 rpm. The resulting supernatant was dried under vacuum, resuspended in 200 ml assay buffer, and serially diluted for insulin measurements with a rat insulin radioimmunoassay kit. Data are presented as means ± SE with P values calculated by Student's t tests.

Northern RNA blots. INS-1 cells were incubated with 20 µmol/l cyclopamine in 0.19% ethanol or 0.19% ethanol carrier for the times indicated. Total RNA was isolated from cells washed in PBS and lysed with Tri-Reagent (Sigma) according to the manufacturer's protocol. For each sample, 4 µg total RNA was separated by electrophoresis on a denaturing gel consisting of 1× MOPS, 1.2% agarose, and 1% formaldehyde. Ethidium bromide staining was used to visualize 28S and 18S RNA. Samples were transferred from gels using standard methods (43) to nylon membranes (Hybond-N+; Amersham Pharmacia Biotech, Piscataway, NJ) and cross-linked with ultraviolet light (UV Stratalinker 1800; Stratagene, La Jolla, CA). The membranes were prehybridized in Rapid-Hyb Buffer (Amersham Pharmacia Biotech) before hybridization for 4 h at 65°C with radiolabeled probes. Insulin transcripts were probed with a 231-nucleotide fragment (spanning nucleotides 349–580 of the rat insulin I gene; GenBank acc. no. V01242) of rat insulin I cDNA. Actin transcripts were probed with a 630-nucleotide cDNA fragment of rat β-actin cDNA (beginning with nucleotide 262 and ending with nucleotide 2371 derived from the rat β-actin gene; GenBank acc. no. V01217). Probes were labeled with [α-^{32}P]-dATP using the RadPrime DNA Labeling System (Gibco). Blots were rinsed in a solution of 0.1× sodium chloride–sodium phosphate (SSC) with 0.1% SDS before autoradiography. Autoradiograms were scanned with a computing densitometer (Molecular Dynamics, Sunnyvale, CA), and individual band intensities were determined with ImageQuant software (Molecular Dynamics).

Immunoprecipitations and Western immunoblots. Transfected or nontransfected INS-1 cells were incubated in fresh culture medium for 24 h before harvesting conditioned medium. Harvested medium was centrifuged at 2,000 rpm for 2 min. For each immunoprecipitation reaction, 1.2 ml of the resulting supernatant was removed, and immunoprecipitations were conducted as described previously (44) in the presence or absence of goat polyclonal IgG anti-Shh COOH-terminus (Shh [C-18]) antiserum (Santa Cruz Biotechnology). Western blot analysis was conducted with primary goat polyclonal IgG anti-Shh COOH-terminus (Shh [C-18]) antiserum (Santa Cruz Biotechnology) and secondary anti-goat IgG-horseradish peroxidase–conjugated antiserum (Santa Cruz Biotechnology) as described (44).

RESULTS

Hh signaling proteins are expressed in pancreatic islets and in clonal INS-1 β-cells. In the adult mouse pancreas, both members of the receptor complex for Hhs, Ptc, and Smo are expressed preferentially in the islets of Langerhans (Fig. 1*A*). Ptc and Smo proteins are expressed in pancreatic β-cells, located within the core of the islet, as demonstrated by their coexpression with insulin. The expression of Ptc in pancreatic β-cells is an indication of the existence of active Hh signaling in pancreatic islets because Ptc is a downstream transcriptional target of the Hh signal transduction pathway, and Ptc expression occurs in response to Hh signaling (17,21,30). Ihh, and less abundantly Dhh, protein expression can be detected as punctate staining within the islet cells of the mouse pancreas (Fig. 1*A*), indicating that autocrine or paracrine interactions of Hh ligands occur with the Hh receptor complex Ptc and Smo within the islets.

Ihh protein is expressed in small highly localized aggregates within pancreatic β-cells. These protein aggregates are not observed when immunostaining is conducted with anti-Ihh antiserum preadsorbed with blocking peptide (data not shown). By confocal microscopy, an average of one or two Ihh protein aggregates of ~1–1.5 µm in diameter are seen per cell, localized in compartments distinct from the insulin secretory granules (Fig. 1*C*). The Ihh protein expression pattern resembles cytoplasmic Hh protein expression in *Drosophila* embryos, described as "punctate," or "dots" (23,33,45). The subcellular aggregates may represent cholesterol raft compartments in which lipid-modified Hh proteins are localized either for the generation or transduction of Hh signals (46–48).

We used the clonal β-cell line INS-1 as a model system of the differentiated pancreatic β-cell in which to study Hh signaling because these cells retain many of the phenotypic characteristics of pancreatic β-cells (41). INS-1 cells express the Hh receptor complex Ptc and Smo, and subpopulations of the INS-1 cells also express Ihh or Dhh (Fig. 1*B*).

Pancreatic islets and INS-1 cells express mRNAs for Hh signaling proteins. Expression of mRNA for the Ptc and Smo receptors and the Hhs Ihh and Dhh was detected in tissue extracts derived from rat islets or INS-1 cells by RT-PCR and confirmed by Southern blotting (Fig. 2). Expression of Shh mRNA was undetected by RT-PCR with primers specific for Shh relative to Dhh or Ihh in cDNA prepared from either rat islets or INS-1 cells (data not shown).

Hh signaling regulates insulin production in INS-1 cells. Because INS-1 cells express Ihh, Dhh, and their receptor complexes Ptc and Smo, we hypothesized that intercellular Hh signaling might be involved in the regulation of β-cell function and insulin production. Therefore, we treated INS-1 cells with cyclopamine, an inhibitor of Hh signaling (37). Insulin secretion was reduced by 40% after 24 h of treatment of the cells with 20 µmol/l cyclopamine (Fig. 3*A*). Cyclopamine also inhibited insulin secretion from INS-1 cells dose dependently (Fig. 3*B*) and reduced insulin content in INS-1 cells by ~40% compared with the insulin content of untreated control cells (Fig. 3*C*), indicating that Hh signaling regulates insulin production. In contrast, short-term administration of cyclopamine to INS-1 cells for 30 or 90 min did not inhibit insulin secretion (data not shown).

Activation of Hh signaling increases the activation of insulin gene transcription in clonal INS-1 β-cells. We used Shh as an established means to activate the Hh signal transduction pathway (28,29,49) to determine whether the observed regulation of insulin production occurs at the transcriptional level. In these studies, we transiently transfected INS-1 cells with a rat insulin I promoter-reporter construct (–410 INS-LUC) (40) and increasing concentrations of an Shh expression plasmid (pShh) to provide an experimental source of Hh. Transfection of the pShh expression vector resulted in the production, secretion, and processing of Shh in the INS-1 cells, as shown by immunoprecipitation of conditioned medium from transfected INS-1 cells with antisera directed against the COOH-terminus of Shh (Fig. 4*A*). Multiple COOH-terminal fragments of Shh were produced that likely differ in posttranslational modifications, including the incorporation of cholesterol and other lipids (22,47).

The addition of the pShh vector increased activation of the insulin promoter in a dose-dependent manner in both clonal INS-1 (Fig. 4*B*) and MIN6 β-cells (Fig. 4*C*), relative to cells transfected with the empty vector pED. In contrast, pShh did not activate the empty reporter vector PXP2 (data not shown). These findings show that activation of the Hh signaling pathway, by the ectopic expression of Shh, increases insulin promoter transcriptional activation in two lines of clonal β-cells. Furthermore, the administration of increasing doses of cyclopamine inhibited the observed Shh-mediated activation of the insulin promoter in a dose-dependent pattern in INS-1 cells (Fig. 4*D*).

Inhibition of endogenous Hh signaling inhibits insulin gene transcription in INS-1 cells. INS-1 cells were then transiently transfected with the –410 INS-LUC promoter-reporter construct without added Hh. The addition of cyclopamine to the transfected INS-1 cells inhibited the basal insulin promoter activity in a dose-dependent manner by up

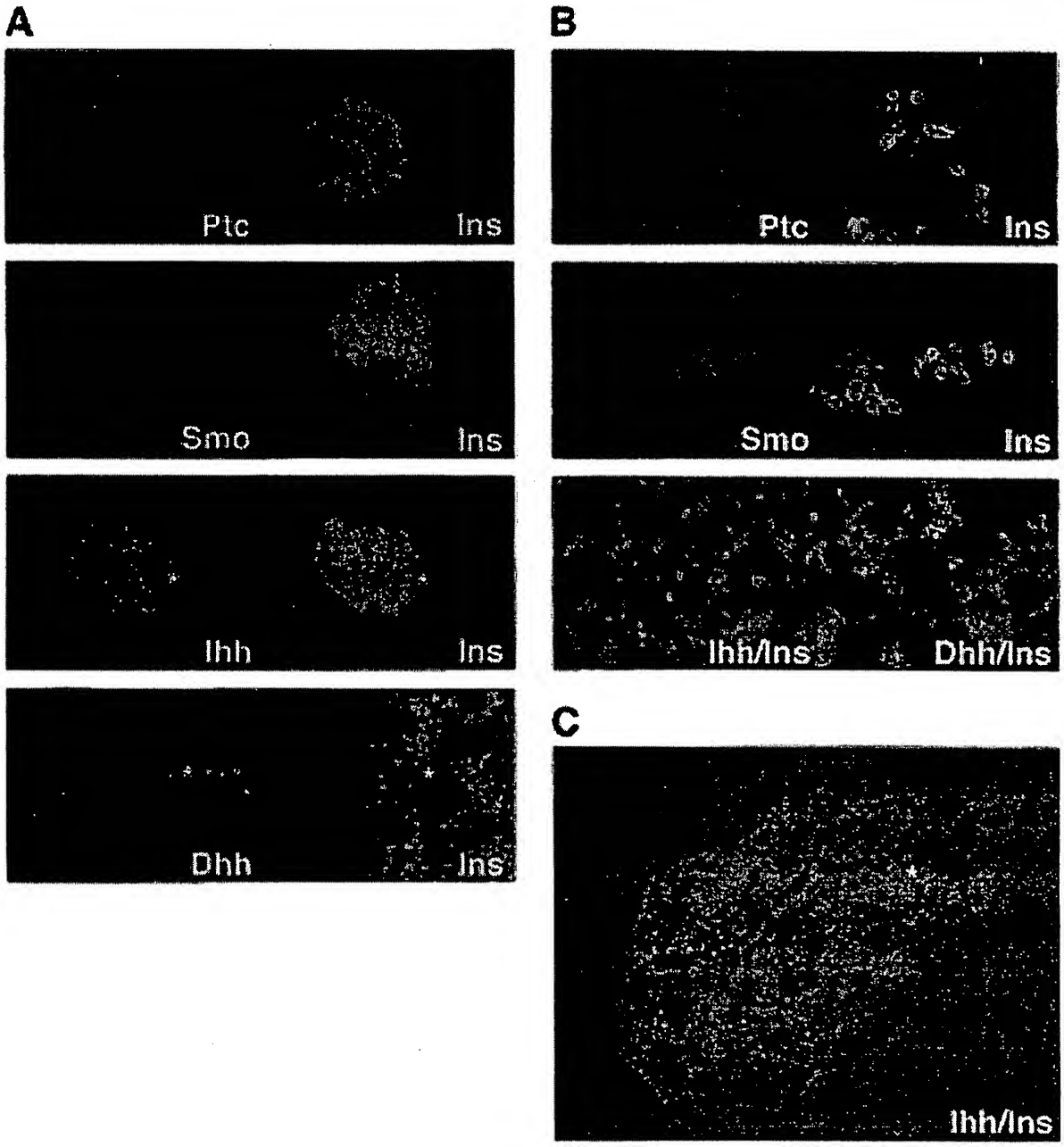

FIG. 1. Expression of Hh signaling proteins in the mouse endocrine pancreas and in insulinoma (INS-1) cells. Immunohistochemical staining of Ihh, Dhh, and Hh receptors Ptc and Smo in adult mouse pancreas (*A*) and in INS-1 cells (*B*). Dual fluorescence immunostaining with antisera to Ihh, Dhh, Ptc, and Smo was developed with the fluorochrome Cy3 (red, left panels) and antiserum to insulin (Ins) with the fluorochrome Cy2 (green, right panels). Asterisks indicate (on left) punctate Ihh or Dhh staining in mouse islets. For Dhh and Ihh in INS-1 cells, dual fluorescence immunostaining was superimposed (right panels) with IP Lab Spectrum (Signal Analytics) software. *C*: Superimposed image of confocal microscopy of dual fluorescence immunostaining of adult mouse pancreas with antisera to Ihh developed with the fluorochrome Cy3 (red punctate pattern) and antiserum to insulin with the fluorochrome Cy2 (green).

to 80% at the highest dose tested. These findings define a range of cyclopamine responsiveness for INS-1 cells (Fig. 5). Therefore, a substantial component of basal insulin promoter activity in INS-1 cells, in the absence of ectopic expression of Hh, is regulated by endogenously produced Hh signaling.

We next examined the effect of inhibiting Hh signaling on the expression of the endogenous insulin gene in INS-1 cells by analyzing insulin mRNA expression. INS-1 cells were treated with 20 μmol/l cyclopamine for 24, 48, and 72 h. Total cellular RNA was prepared and was analyzed by Northern RNA

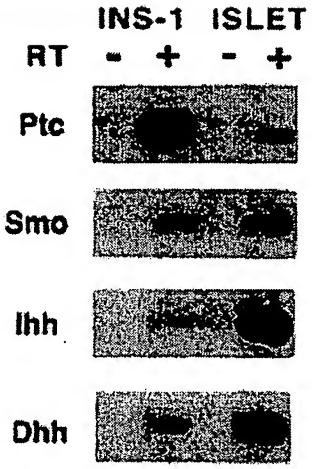

FIG. 2. Expression of mRNA for Hh signaling proteins in rat pancreatic islets and the INS-1 β-cell line. cDNA was prepared from total RNA derived from rat islets or INS-1 cells in the presence (+) or absence (–) of RT and amplified with primers directed toward Ptc, Smo, Ihh, and Dhh. The PCR fragments were the expected sizes of 266, 372, 387, and 331 bp, respectively. Autoradiograms are shown of the corresponding Southern blots probed with [^{32}P]-labeled oligonucleotide probes targeting segments of sequence internal to each set of PCR primers.

blot analysis. Relative insulin-to-actin mRNA levels for cyclopamine-treated cells were similar to the relative levels found in untreated control cells at 24 and 48 h. However, after 72 h of exposure to cyclopamine, relative insulin-to-actin RNA levels were 55% of those observed for untreated control cells (Figs. 6*A* and *B*). The time required for the inhibition of endogenous insulin gene expression by cyclopamine was longer than that required for the inhibition of the activation of transfected insulin promoter constructs, likely because of the long half-life (~25 h) of insulin mRNA (50). The treatment of INS-1 cells with cyclopamine for 72 h also reduced insulin mRNA levels relative to 28S and 18S RNAs (Fig. 6*C*), confirming the importance of active Hh signaling in the maintenance of insulin gene expression in insulin-producing cells.

DISCUSSION

Studies of Hh signaling have focused on the early developmental programs of tissue patterning of the pancreas. Our studies now indicate that Hhs also regulate gene expression in the fully differentiated pancreas. We show that Hh signaling stimulates the expression of the insulin gene in insulin-producing cells. Our findings that Ihh and Dhh and their receptors Ptc and Smo are expressed in the endocrine pancreas support a model in which Hh signaling actively modulates islet cell function in the fully developed adult pancreas. In particular, this hypothesis is strengthened by our demonstration of expression in pancreatic islets of Ptc, a downstream target of transcriptional activation in response to active signaling by Shh, Dhh, or Ihh (17,21,30). It is important to note that the expression of Ptc is taken as an indicator of the existence of ongoing active Hh signaling. In Hh-mediated developmental patterning, local expression of Ptc correlates with neighboring expression of Shh, Ihh, or Dhh (21,29,30). Ectopic expression of Hhs in *Drosophila*, chick embryos, and transgenic mouse models induces ectopic Ptc expression (29,30,33,

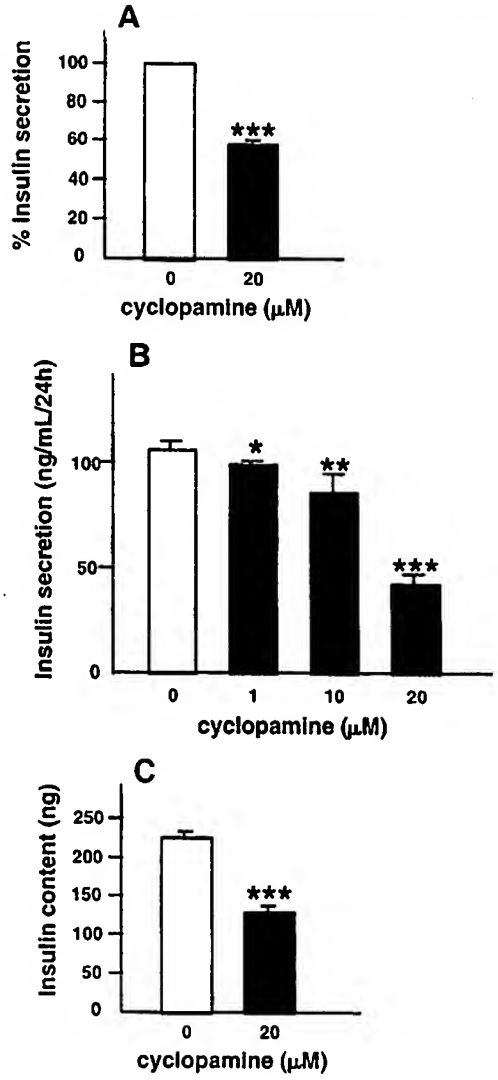

FIG. 3. Cyclopamine, an inhibitor of Hh signaling, inhibits insulin secretion and decreases insulin content in INS-1 cells. *A*: Cyclopamine inhibits insulin secretion from INS-1 cells. INS-1 cells were incubated with 0.19% ethanol (carrier control) or 20 μmol/l cyclopamine in 0.19% ethanol for 24 h at 37°C before collection of aliquots of culture medium for insulin radioimmunoassay. Results shown are the mean ± SE of seven determinations (n = 7), each assayed in duplicate, derived from three distinct passages of INS-1 cells. For each passage of INS-1 cells tested, percent insulin secretion was determined by comparing the mean insulin secretion from cyclopamine-treated cells with the mean insulin secretion of control cells that was designated as 100%. *B*: Cyclopamine inhibits insulin secretion from transfected INS-1 cells in a dose-dependent manner. INS-1 cells transfected for the experiments shown in Fig. 4*D* that were treated with cyclopamine were also used for insulin secretion studies. Aliquots of culture medium were collected from INS-1 cells 24 h after transfection with the empty reporter vector pXP2 and the empty expression vector pED and treatment with 0, 1, 10, or 20 μmol/l cyclopamine in 0.19% ethanol as described in RESEARCH DESIGN AND METHODS. Insulin levels were measured by radioimmunoassay. Results shown are the mean ± SE of two determinations (n = 2), each assayed in duplicate. *C*: Cyclopamine decreases insulin content of INS-1 cells. INS-1 cells were incubated with 0.19% ethanol (carrier control) or 20 μmol/l cyclopamine in 0.19% ethanol for 24 h at 37°C before acid ethanol extraction and radioimmunoassay for insulin. Results shown are the mean ± SE of two determinations (n = 2), each assayed in duplicate. *P < 0.10; **P < 0.05; ***P < 0.01.

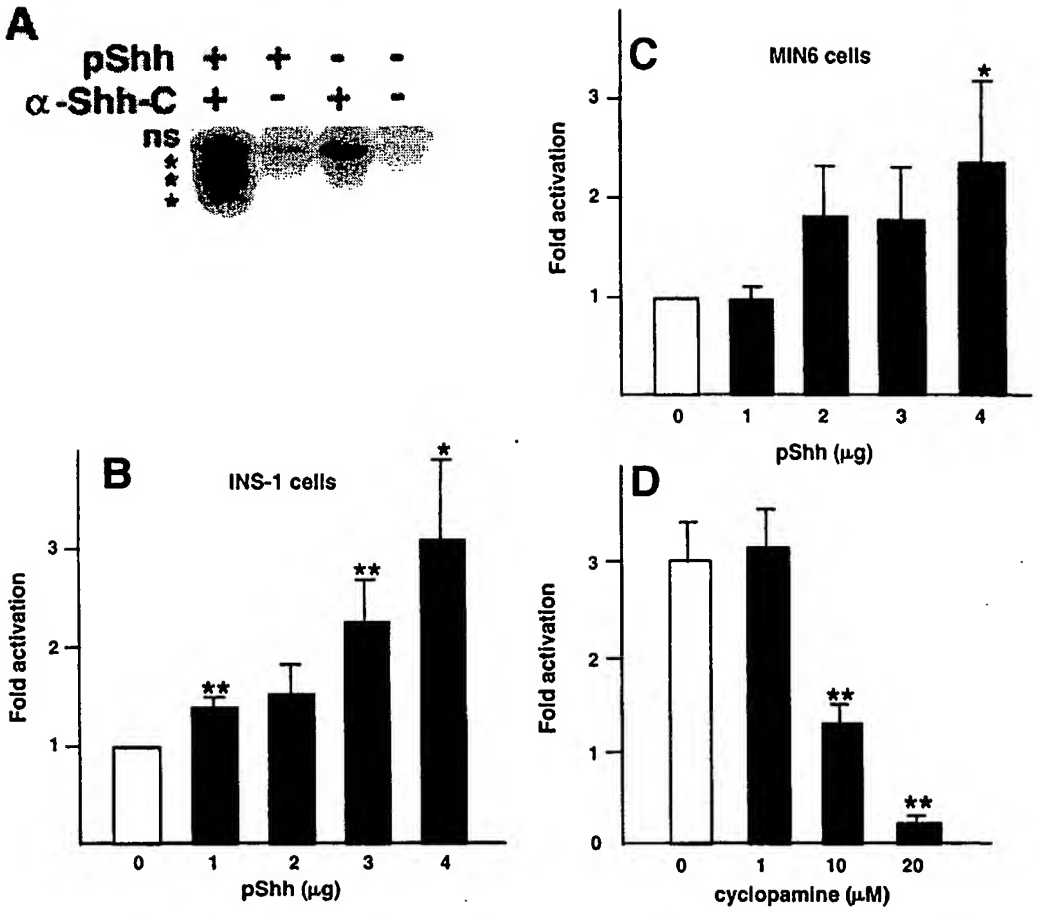

FIG. 4. Activation of Hh signaling via ectopic expression of Shh increases transcriptional activation of the rat insulin I promoter in INS-1 cells. *A*: INS-1 cells transfected with pShh process and secrete Shh. INS-1 cells were transiently transfected with 4 μg pED empty vector (–, top row) or 4 μg pShh (+, top row) as indicated. After 24 h of culture at 37°C, conditioned medium from transfected INS-1 cells was collected and subjected to immunoprecipitation with (+, bottom row) or without (–, bottom row) goat polyclonal anti-Shh COOH-terminus (αShh-C) antiserum and analyzed by Western blotting with anti-Shh COOH-terminus antiserum. The COOH-terminal fragment of Shh migrated as multiple bands near the expected molecular weight of 27 kDa as indicated by asterisks. A nonspecific band seen by Western blotting is designated (ns). Shh activates the promoter of the rat insulin I gene in INS-1 cells (*B*) or MIN6 cells (*C*) in a dose-dependent manner. The cells were transiently cotransfected with 2 μg of the transcriptional reporter plasmid –410INS-LUC or the empty reporter plasmid pXP2 (data not shown) and 0–4 μg pShh with 4–0 μg pED empty vector as indicated. Cells were harvested after 24 h, and luciferase activities were determined and normalized with protein concentrations of the cell extracts. Fold-activation was determined by comparing luciferase activity (luciferase units per microgram protein) at each point within a transfection to the activity of the pED empty vector (0) that was designated as 100%. pShh did not activate the empty reporter plasmid pXP2 (data not shown). Results shown are the mean ± SE of three independent cell transfection experiments (n = 3), each conducted in duplicate. *D*: Cyclopamine inhibits activation of the rat insulin I promoter by ectopic expression of Shh in INS-1 cells. INS-1 cells were transiently transfected with 2 μg of the transcriptional reporter plasmid –410INS-LUC and 4 μg pShh or 4 μg pED (data not shown). Cyclopamine administration was conducted as described in RESEARCH DESIGN AND METHODS. Fold-activation was determined by normalizing luciferase activity (luciferase units per microgram protein) at each point within a transfection to the activity of pED in the absence of cyclopamine treatment that was designated as 100%. Results shown are the mean ± SE of three transfections (n = 3), each conducted with duplicate samples. *P < 0.10; **P < 0.05.

51–53). Mutations or disruptions of Hhs result in decreased Ptc expression in target tissues (17,21,51). In particular, Ptc expression is not detected in the skeleton of Ihh knockout mice, in contrast to the normal pattern of Ptc expression in proliferating chondrocytes (17). Targeted disruption of Dhh in male mice results in the loss of Ptc expression normally seen in Sertoli cells (21). There are multiple potential endogenous activators of Hh signal transduction in pancreatic β-cells. Ihh and Dhh signals appear to be more important local activators of the Hh signaling pathway in vivo in differentiated pancreatic islets because we did not detect expression of Shh in pancreatic β-cells.

The activation of the insulin promoter by an exogenous activator of Hh signaling and the repression of promoter activity by the Hh signaling inhibitor cyclopamine implicate the insulin gene as a target for positive regulation by Hhs in pancreatic β-cells. The activation of the insulin promoter by Hh signaling may be interpreted as unexpected or even surprising in light of experimental evidence suggesting that early pancreas development requires the absence of Shh expression (34–36,38). However, Hh mRNA expression in developing systems does not necessarily reflect the extent of local Hh signaling because, in tissues, Hh morphogens can travel substantial distances from their sites of production (24). More-

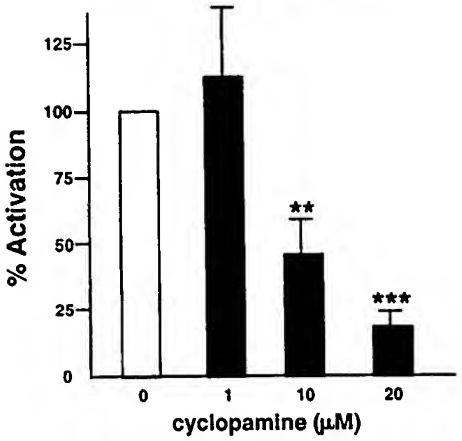

FIG. 5. Cyclopamine decreases activation of the rat insulin I promoter by endogenous Hh expression in INS-1 cells. INS-1 cells were transiently transfected with 2 μg of the transcriptional reporter plasmid –410INS-LUC and 4 μg pED empty vector and treated with cyclopamine as in the experiments shown in Fig. 4*D*. Fold-activation was determined by normalizing luciferase activity (luciferase units per microgram protein) at each point within a transfection to the activity of pED in the absence of cyclopamine treatment that was designated as 100%. Results shown are the mean ± SE of three transfections (n = 3), each conducted with duplicate samples. *P < 0.10; **P < 0.05.

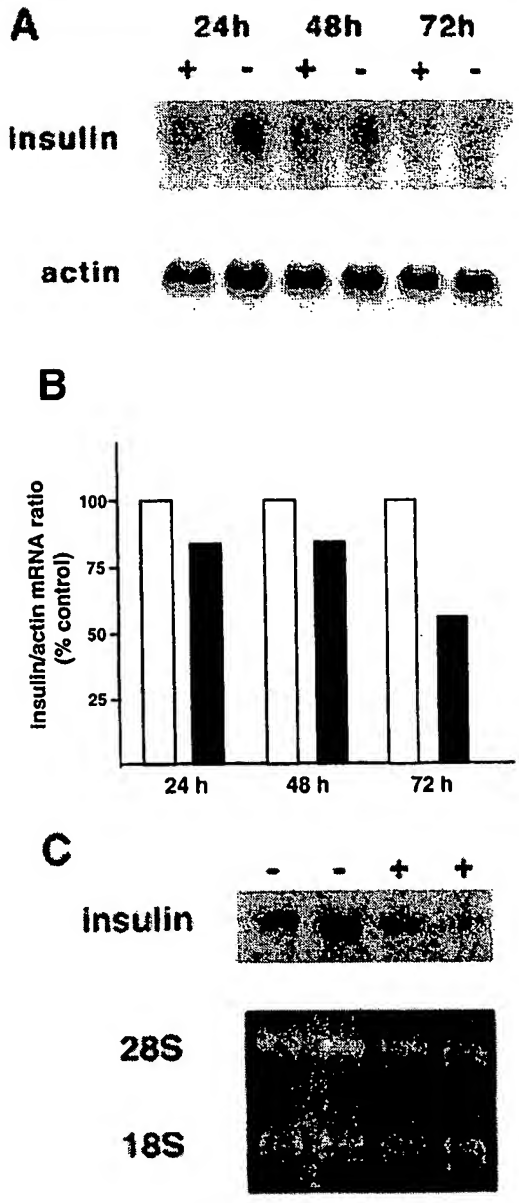

FIG. 6. Cyclopamine decreases endogenous insulin mRNA expression in INS-1 cells. *A*: INS-1 cells were cultured with 0.19% ethanol (control) (–) or 20 μmol/l cyclopamine in 0.19% ethanol (+). Culture medium was changed twice daily for a total incubation period of 24, 48, or 72 h. Total RNA was extracted from the cells and analyzed by Northern blotting for rat insulin I (upper panel) and β-actin (lower panel) transcripts. The corresponding autoradiograms are shown. *B*: Scanning densitometry of autoradiograms from the data shown in Fig. 5*A*. For each time point, signal intensities were determined for insulin and actin transcripts. The relative intensity of insulin transcript to actin transcript was determined as an insulin/actin ratio for the control sample at each time point. Insulin/actin ratios for cyclopamine-treated samples are shown relative to each corresponding control set at 100%. □, Control; ■, cyclopamine. *C*: Duplicate samples of INS-1 cells were cultured with 0.19% ethanol (–) or 20 μmol/l cyclopamine in 0.19% ethanol (+). Culture medium was changed daily for a total incubation period of 72 h. Total RNA was extracted from the cells and analyzed by Northern blotting for rat insulin I (upper panel). A photograph of the corresponding ethidium bromide-stained agarose gel showing levels of 28S and 18S ribosomal RNA is shown (lower panel).

over, it is well known that developmental morphogens can be either activators or repressors of gene transcription depending on the local ambient concentrations of the morphogens and the previous temporal experience of the cells to other morphogens. The differences in levels of Hh expression noted in the embryonic foregut from which the pancreas develops may reflect active Hh signaling that participates in the formation of boundaries for the developing pancreas in a manner analogous to wing patterning in *Drosophila* or in butterflies (54). Such a model is supported by Shh and Ihh knockout mouse models that exhibit pancreatic phenotypes (55). The developmental studies of Hh signaling in the pancreas do not preclude coincident Hh signaling and insulin gene expression. In the transgenic mouse model in which Shh was overexpressed in pancreatic β-cells, insulin expression was retained although pancreas morphology was markedly abnormal (34).

The differences observed in Hh function in developing and differentiated systems may reflect the complex regulation of Hh signaling pathways. Hh signaling can activate or repress gene transcription, depending on the regulation of multiple isoforms of the Gli/Ci transcription factors (56,57). Local concentrations of Ptc receptors may favor either sequestration or transmission of Hh signals (58). The multiple forms of vertebrate Hhs, two of which (Ihh and Dhh) are expressed in the pancreatic islet, may also regulate distinct processes in the same tissues at different times in development, as illustrated by Shh in the regulation of early limb bud development, followed by Ihh in the regulation of cartilage differentiation at later stages of skeletal development (29,30).

Like Hhs, other factors have different actions in pancreas development than in differentiated pancreatic β-cells. For example, expression of the pancreas-specific homeoprotein pancreas duodenum homeobox-1 (PDX-1) is required for the development of both the exocrine and the endocrine pancreas

(59,60). However, later in development, expression of PDX-1 is restricted primarily to the differentiated pancreatic β-cells within the endocrine pancreas wherein it regulates expression of β-cell–specific genes, including insulin, GLUT2, and glucokinase (61). The transcription factors Isl-1, Pax4, Pax6, Nkx2.2, Nkx6.1, and Beta2/NeuroD are essential for the development of the endocrine pancreas but are also important transcriptional regulators in differentiated pancreatic endocrine cells (62).

Our data suggest that the intercellular Hh signaling machinery that is implicated in pattern formation in the early development of the pancreas is deployed later by fully differentiated pancreatic β-cells for the regulation of insulin gene expression. It is possible that paracrine Hh signaling among neighboring β-cells and non–β-cells in the islets coordinates insulin production and that autocrine Hh signaling is part of a regulatory loop within these cells. Ihh protein is highly localized in a punctate pattern within β-cells, a distribution similar to that of *Drosophila* Hh (23,33,45), which is consistent with the proposed localization of Hh proteins within cholesterol rafts (47,48). This finding is of particular interest, since cholesterol modification regulates the transcellular movement of Hh ligands for long-range actions (23–25).

The regulation of insulin production by Hh signals may occur through multiple mechanisms. Inhibition of Hh signaling in INS-1 cells diminished insulin content more rapidly than insulin mRNA transcripts declined—a decline likely delayed by the long half-life of insulin mRNA. Although we did not observe an independent effect of Hh signaling on short-term insulin secretion, in addition to effects on insulin gene transcription, Hh signals may regulate insulin production at other levels, including mRNA translation, post-translational processing, or protein stability.

Hh proteins, as potential regulators of insulin production in the endocrine pancreas, may be relevant to the pathogenesis and treatment of diabetes or hyperinsulinism. Because pancreatic β-cells produce insufficient levels of insulin to maintain normal glucose homeostasis in adult-onset diabetic patients, defective Hh signaling conceivably may be part of the pathogenetic process in type 2 diabetes. The identification of the insulin gene as a target of Hh signaling may stimulate the development of novel strategies for the regulation of insulin levels in disease states.

ACKNOWLEDGMENTS

These studies were supported by grants DK30834, DK55365, DK30457 (J.F.H.), and DK02476 (M.K.T.) from the National Institutes of Health. J.F.H. is an Investigator with the Howard Hughes Medical Institute.

We thank A. McMahon for mouse Shh cDNA, C.P. Miller for pED vectors, W. Gaffield for cyclopamine, C. Wollheim for INS-1 cells, and J. Miyazaki for MIN6 cells. We appreciate the expert technical assistance of D. Brown, K. McManus, and H. Hermann. We also thank T. Budde and R. Larraga for their assistance in the preparation of this manuscript.

REFERENCES

1. Nusslein-Volhard C, Wieschaus E: Mutations affecting segment number and polarity in *Drosophila*. *Nature* 287:795–801, 1980
2. Mohler J: Requirements for hedgehog, a segment polarity gene, in patterning larval and adult cuticle of *Drosophila*. *Genetics* 120:1988, p.1061-1072.
3. Forbes AJ, Nakano Y, Taylor AM, Ingham PW: Genetic analysis of hedgehog signaling in the *Drosophila* embryo. *Dev Suppl* 115–124, 1993
4. Basler K, Struhl G: Compartment boundaries and the control of *Drosophila* limb pattern by hedgehog protein. *Nature* 368:208–214, 1994
5. Diaz-Benjumea FJ, Cohen SM: Cell-interaction between compartments establishes the proximal-distal axis of *Drosophila* legs. *Nature* 372:175–179, 1994
6. Zecca M, Basler K, Struhl G: Sequential organizing activities of engrailed, hedgehog and decapentaplegic in *Drosophila* wing. *Dev Suppl* 121:2265–2278, 1995
7. Blair S, Ralston A: Smoothened-mediated hedgehog signaling is required for the maintenance of the anterior-posterior lineage restriction in the developing wing of *Drosophila*. *Development* 124:4053–4063, 1997
8. Rodriguez I, Basler K: Control of compartmental affinity boundaries by hedgehog. *Nature* 389:614–618, 1997
9. Hammerschmidt M, Brook A, McMahon AP: The world according to hedgehog. *Trends Genet* 13:14–21, 1997
10. Weed M, Mundlos S, Olsen BR: The role of sonic hedgehog in vertebrate development. *Matrix Biol* 16:53–58, 1997
11. Pepicelli CV, Lewis PM, McMahon AP: Sonic hedgehog regulates branching morphogenesis in the mammalian lung. *Curr Biol* 8:1083–1086, 1998
12. Briscoe J, Ericson J: The specification of neuronal identity by graded sonic hedgehog signalling. *Semin Cell Dev Biol* 10:353–362, 1999
13. Ryan AK, Blumberg B, Rodriguez-Esteban C, Yonei-Tamura S, Tamura K, Tsukui T, de la Pena J, Sabbagh W, Greenwald J, Choe S, Norris DP, Robertson EJ, Evans RE, Rosenfeld MG, Belmonte JCI: Pitx2 determines left-right asymmetry of internal organs in vertebrates. *Nature* 394:545–551, 1998
14. Piedra ME, Icardo JM, Albajar MA, Rodriguez-Rey JC, Ros MA: Pitx2 participates in the late phase of the pathway controlling left-right asymmetry. *Cell* 94:319–324, 1998
15. Logan M, Pagan-Westphal SM, Smith DM, Paganessi L, Tabin CJ: The transcription factor Pitx2 mediates situs-specific morphogenesis in response to left-right asymmetric signals. *Cell* 94:307–318, 1998
16. Yoshioka H, Meno C, Koshiba K, Sugihara M, Itoh H, Ishimaru Y, Inoue T, Ohuchi H, Semina E, Murray JC, Hamada H, Noji S: Pitx2, a bicoid-type homeobox gene, is involved in a lefty-signaling pathway in determination of left-right asymmetry. *Cell* 94:299–305, 1998
17. St-Jacques B, Hammerschmidt M, McMahon AP: Indian hedgehog signaling regulates proliferation and differentiation of chondrocytes and is essential for bone formation. *Genes Dev* 13:2072–2086, 1999
18. Karp SJ, Schipani E, St-Jacques B, Hunzelman J, Kronenberg H, McMahon AP: Indian Hedgehog coordinates endochondral bone growth and morphogenesis via parathyroid hormone related-protein-dependent and -independent pathways. *Development* 127:543–548, 2000
19. Lewis MT, Ross S, Strickland PA, Sugnet CW, Jimenez E, Scott MP, Daniel CW: Defects in mouse mammary gland development caused by conditional haploinsufficiency of Patched-1. *Development* 126:5181–5193, 1999
20. Parmantier E, Lynn B, Lawson D, Turmaine M, Namini SS, Chakrabarti L, McMahon AP, Jessen KR, Mirsky R: Schwann cell-derived Desert hedgehog controls the development of peripheral nerve sheaths. *Neuron* 23:713–724, 1999
21. Bitgood MJ, Shen L, McMahon AP: Sertoli cell signaling by Desert hedgehog regulates the male germline. *Curr Biol* 6:298–304, 1996
22. Porter JA, Young KE, Beachy PA: Cholesterol modification of hedgehog signaling proteins in animal development. *Science* 274:255–259, 1996
23. Bellaiche Y, The I, Perrimon N: Tout-velu is a *Drosophila* homologue of the putative tumour suppressor EXT-1 and is needed for Hh diffusion. *Nature* 394:85–88, 1998
24. Burke R, Nellen D, Bellotto M, Hafen E, Senti KA, Dickson BJ, Basler K: Dispatched, a novel sterol-sensing domain protein dedicated to the release of cholesterol-modified hedgehog from signaling cells. *Cell* 99:803–815, 1999
25. The I, Bellaiche Y, Perrimon N: Hedgehog movement is regulated through tout velu-dependent synthesis of a heparan sulfate proteoglycan. *Mol Cell* 4:633–639, 1999
26. Stone DM, Hynes M, Armanini M, Swanson TA, Gu Q, Johnson RL, Scott MP, Pennica D, Goddard A, Phillips H, Noll M, Hooper JE, de Sauvage F, Rosenthal A: The tumor-suppressor gene patched encodes a candidate receptor for Sonic hedgehog. *Nature* 384:129–134, 1996
27. Ingham PW: Transducing hedgehog: the story so far. *EMBO J* 17:3505–3511, 1998
28. Krishnan V, Pereira F, Qiu Y, Chen C, Beachy P, Tsai S, Tsai M: Mediation of Sonic hedgehog induced expression of COUP-TFII by a protein phosphatase. *Science* 278:1947–1950, 1997
29. Vortkamp A, Lee K, Lanske B, Segre GV, Kronenberg HM, Tabin CJ: Regulation of rate of cartilage differentiation by Indian hedgehog and PTH-related protein. *Science* 273:613–621, 1996
30. Goodrich LV, Johnson RL, Milenkovic L, McMahon JA, Scott MP: Conservation of the hedgehog/patched signaling pathway from flies to mice: induction of a mouse patched gene by Hedgehog. *Genes Dev* 10:301–312, 1996

31. Alexandre C, Jacinto A, Ingham PW: Transcriptional activation of hedgehog target genes in *Drosophila* is mediated directly by the Cubitus interruptus protein, a member of the GLI family of zinc finger DNA-binding proteins. *Genes Dev* 10:2003–2013, 1996
32. Hidalgo A, Ingham P: Cell patterning in the *Drosophila* segment: spatial regulation of the segment polarity gene patched. *Development* 110:291–301, 1990
33. Tabata T, Kornberg TB: Hedgehog is a signaling protein with a key role in patterning *Drosophila* imaginal discs. *Cell* 76:89–102, 1994
34. Apelqvist A, Ahlgren U, Edlund H: Sonic hedgehog directs specialised mesoderm differentiation in the intestine and pancreas. *Curr Biol* 7:801–804, 1997
35. Kim SK, Hebrok M, Melton DA: Notochord to endoderm signaling is required for pancreas development. *Development* 124:4243–4252, 1997
36. Hebrok M, Kim SK, Melton DA: Notochord repression of endodermal sonic hedgehog permits pancreas development. *Genes Dev* 12:1705–1713, 1998
37. Cooper MK, Porter JA, Young KE, Beachy PA: Teratogen-mediated inhibition of target tissue response to Shh signaling. *Science* 280:1603–1607, 1998
38. Kim SK, Melton DA: Pancreas development is promoted by cyclopamine, a Hedgehog signaling inhibitor. *Proc Natl Acad Sci U S A* 95:13036–13041, 1998
39. Kaufman RJ, Davies MV, Wasley LC, Michnick D: Improved vectors for stable expression of foreign genes in mammalian cells by use of the untranslated leader sequence from EMC virus. *Nucleic Acids Res* 19:4485–4490, 1991
40. Lu M, Seufert J, Habener JF: Pancreatic β-cell-specific repression of insulin gene transcription by CCAAT/enhancer-binding protein β. *J Biol Chem* 272: 28349–28359, 1997
41. Asfari M, Janjic D, Meda P, Li G, Halban PA, Wollheim CB: Establishment of 2-mercaptoethanol-dependent differentiated insulin-secreting cell lines. *Endocrinology* 130:167–178, 1992
42. Miyazaki J, Araki K, Yamato E, Ikegami H, Asano T, Shibasaki Y, Oka Y, Yamamura K: Establishment of a pancreatic beta cell line that retains glucose-inducible insulin secretion: special reference to expression of glucose transporter isoforms. *Endocrinology* 127:126–132, 1990
43. Ausubel FM, Brent R, Kingston RE, Moore DD, Seidman JG, Smith JA, Struhl K: *Current Protocols in Molecular Biology.* Vol. 2. New York, Wiley, 1994
44. Thomas MK, Yao KM, Tenser MS, Wong GG, Habener JF: Bridge-1, a novel PDZ-domain coactivator of E2A-mediated regulation of insulin gene transcription. *Mol Cell Biol* 19:8492–8404, 1999
45. Taylor AM, Nakano Y, Mohler J, Ingham PW: Contrasting distributions of patched and hedgehog proteins in the *Drosophila* embryo. *Mech Devel* 42:89–96, 1993
46. Pepinsky RB, Zeng C, Wen D, Rayhorn P, Baker DP, Williams KP, Bixler SA, Ambrose CM, Garber EA, Miatkowski K, Taylor FR, Wang EA, Galdes A: Identification of a palmitic acid-modified form of human sonic hedgehog. *J Biol Chem* 273:14037–14045, 1998
47. Rietveld A, Neutz S, Simons K, Eaton S: Association of sterol- and glycosylphophatidylinositol-linked proteins with *Drosophila* raft lipid microdomains. *J Biol Chem* 274:12049–12054, 1999
48. Incardona JP, Eaton S: Cholesterol in signal transduction. *Curr Opin Cell Biol* 12:193–203, 2000
49. Lanske B, Karaplis AC, Lee K, Luz A, Vortkamp A, Pirro A, Karperien M, Defize LHK, Ho C, Mulligan RC, Abou-Samra AB, Juppner H, Segre GV, Kronenberg HM: PTH/PTHrP receptor in early development and Indian hedgehog-regulated bone growth. *Science* 273:663–666, 1996
50. Welsh M, Nielsen DA, MacKrell AJ, Steiner DF: Control of insulin gene expression in pancreatic beta-cells and in an insulin-producing cell line, RIN-5F cells. II. Regulation of insulin mRNA stability. *J Biol Chem* 260:13590–13594, 1985
51. Capdevila J, Pablo Estrada M, Sanchez-Herrero E, Guerrero I: The *Drosophila* segment polarity gene patched interacts with decapentaplegic in wing development. *EMBO J* 13:71–82, 1994
52. Marigo B, Scott MP, Johnson RL, Goodrich LV, Tabin CJ: Conservation in hedgehog signaling: induction of a chicken patched homolog by Sonic hedgehog in the developing limb. *Development* 122:1225–1233, 1996
53. Marigo V, Tabin CJ: Regulation of patched by sonic hedgehog in the developing neural tube. *Proc Natl Acad Sci U S A* 93:9346–9351, 1996
54. Keys DN, Lewis DL, Selegue JE, Pearson BJ, Goodrich LV, Johnson RL, Gates JG, Scott MP, Carroll SB: Recruitment of a hedgehog regulatory circuit in butterfly eyespot evolution. *Science* 283:532–534, 1999
55. Ramalho-Santos M, Melton DA, McMahon AP: Hedgehog signals regulate multiple aspects of gastrointestinal development. *Development* 127:2763–2772, 2000
56. Methot N, Basler K: Hedgehog controls limb development by regulating the activities of distinct transcriptional activator and repressor forms of Cubitus interruptus. *Cell* 96:819–831, 1999
57. Altaba AR: Gli proteins encode context-dependent positive and negative functions: implications for development and disease. *Development* 126:3205–3216, 1999
58. Chen Y, Struhl G: Dual roles for patched in sequestering and transducing Hedgehog. *Cell* 87:553–563, 1996
59. Jonsson J, Carlsson L, Edlund T, Edlund H: Insulin-promoter-factor 1 is required for pancreas development in mice. *Nature* 371:606–609, 1994
60. Offield MF, Jetton TL, Labosky PA, Ray M, Stein RW, Magnuson MA, Hogan BLM, Wright CVE: PDX-1 is required for pancreatic outgrowth and differentiation of the rostral duodenum. *Development* 122:983–995, 1996
61. Stoffers DA, Thomas MK, Habener JF: Homeodomain protein IDX-1: a master regulator of pancreas development and insulin gene expression. *Trends Endocrinol Metab* 8:145–151, 1997
62. Edlund H: Transcribing pancreas. *Diabetes* 47:1817–1823, 1998

ELSEVIER

Mechanisms of Development 106 (2001) 143–145

www.elsevier.com/locate/modo

Gene expression pattern

Shh and *Ptc* are associated with taste bud maintenance in the adult mouse

Hirohito Miura[a,c,*], Yuko Kusakabe[a,c], Chiaki Sugiyama[a], Michiko Kawamatsu[c], Yuzo Ninomiya[b,c], Jun Motoyama[d], Akihiro Hino[a,c]

[a]*National Food Research Institute, 2-1-12 Kannondai, Tsukuba-shi, Ibaraki 305-8642, Japan*
[b]*Faculty of Dentistry, Kyushu University, 3-1-1 Maidashi Higashi-ku, Fukuoka-shi, Fukuoka 812-8582, Japan*
[c]*Bio-oriented Technology Research Advancement Institution (BRAIN), 3-18-19 Toranomon Minato-ku, Tokyo 105, Japan*
[d]*Molecular Neuropathology Group, Brain Science Institute, The Institute of Physical and Chemical Research (RIKEN), 2-1 Hirosawa, Wako, Saitama, 351-0198, Japan*

Received 9 February 2001; received in revised form 3 April 2001; accepted 25 April 2001

Abstract

In mammals, taste receptor cells are organized into taste buds on tongue. Taste buds are trophically maintained by taste neurons and under continuous renewal, even in adults. We found that the receptor for *Sonic hedgehog* (*Shh*), *Patched1* (*Ptc*), was expressed around taste buds where cells were proliferating, and that *Shh* was expressed within basal cells of taste buds. Denervation caused the loss of *Shh* and *Ptc* expression before the degeneration of taste buds. © 2001 Elsevier Science Ireland Ltd. All rights reserved.

Keywords: Taste bud; Tongue; Taste nerve; Sonic hedgehog; Patched1; Adult mouse

1. Results

Ptc is a conserved target of Shh signaling; its expression can indicate the tissues responding to Shh during development (Goodrich et al., 1996; Marigo et al., 1996). *Shh* and *Ptc* were reported to be expressed in developing taste papillae in the embryonic stage, suggesting that Shh is involved in the morphogenesis of taste papillae (Hall et al., 1999; Jung et al., 1999). Here we report the expression of *Shh* and *Ptc* in lingual epithelium of the adult mouse.

Taste buds in the tongue are localized in three types of taste papilla, the circumvallate, foliate and fungiform papillae. In circumvallate papillae, the expression of *Ptc* was found in epithelial cells on the basal side adjacent to each taste bud but not in the taste buds (Fig. 1A). In contrast, *Shh* was expressed in limited basal cells within the taste buds (Fig. 1B). The same expression pattern of *Shh* was observed in fungiform and foliate papillae (Fig. 1C and data not shown). *Ptc* and *Shh* expression in the tongue was restricted to local epithelium containing taste buds, and the expression was not detectable in the other epithelial regions or underlying mesenchyme (Fig. 1D,E). In sagittal sections, *Ptc* expression was found to be present in the basal but not in the apical region surrounding the taste buds (Fig. 1F). *Shh* expression in basal cells was enclosed by the *Ptc*-expressing region (Fig. 1G).

Cells within a taste bud undergo continual turnover, even in the adult tongue. The studies following [^{3}H]thymidine incorporation have shown that epithelial cells surrounding the taste bud divide, and that some of the daughter cells enter the taste bud (Beidler and Smallman, 1965; Farbman, 1980; Delay et al., 1986). We injected BrdU to label proliferating cells and compared the distribution of BrdU-labeled cells with the *Ptc* expression pattern. At 24 h after BrdU injection, BrdU-labeled cells occurred around the taste buds in epithelia of circumvallate papillae and the distribution of BrdU-labeled cells was included within the *Ptc*-expressing regions surrounding taste buds (Fig. 2A–F). At 5.5 days after BrdU injection, BrdU-labeled cells were evident within taste buds, suggesting that proliferating cells around taste buds had migrated into the taste buds (Fig. 2G).

We next crushed the right glossopharyngeal nerve (IXth) and compared the expressions of *Ptc* and *Keratin8* in circumvallate papillae in serial adjacent sections, using the left trench as a control. Taste buds in circumvallate papillae are innervated by IXth nerve and disappear at about 8 days after the nerve crush (Smith et al., 1994). *Keratin8* is expressed in taste buds, so the signal for *Keratin8* indicates remaining taste cells (Zhang et al., 1997). Four days after the right IXth nerve crush, the expression of *Ptc* had almost disappeared in the right trench, while the expression of *Keratin8* was noted (Fig. 3). The *Shh* expression, like *Ptc*, had disappeared in taste buds after denervation (data not

* Corresponding author. Tel.: +81-298-38-8079; fax: +81-298-38-7996.
E-mail address: hmiura@nfri.affrc.go.jp (H. Miura).

PII: S0925-4773(01)00414-2

EXHIBIT 4

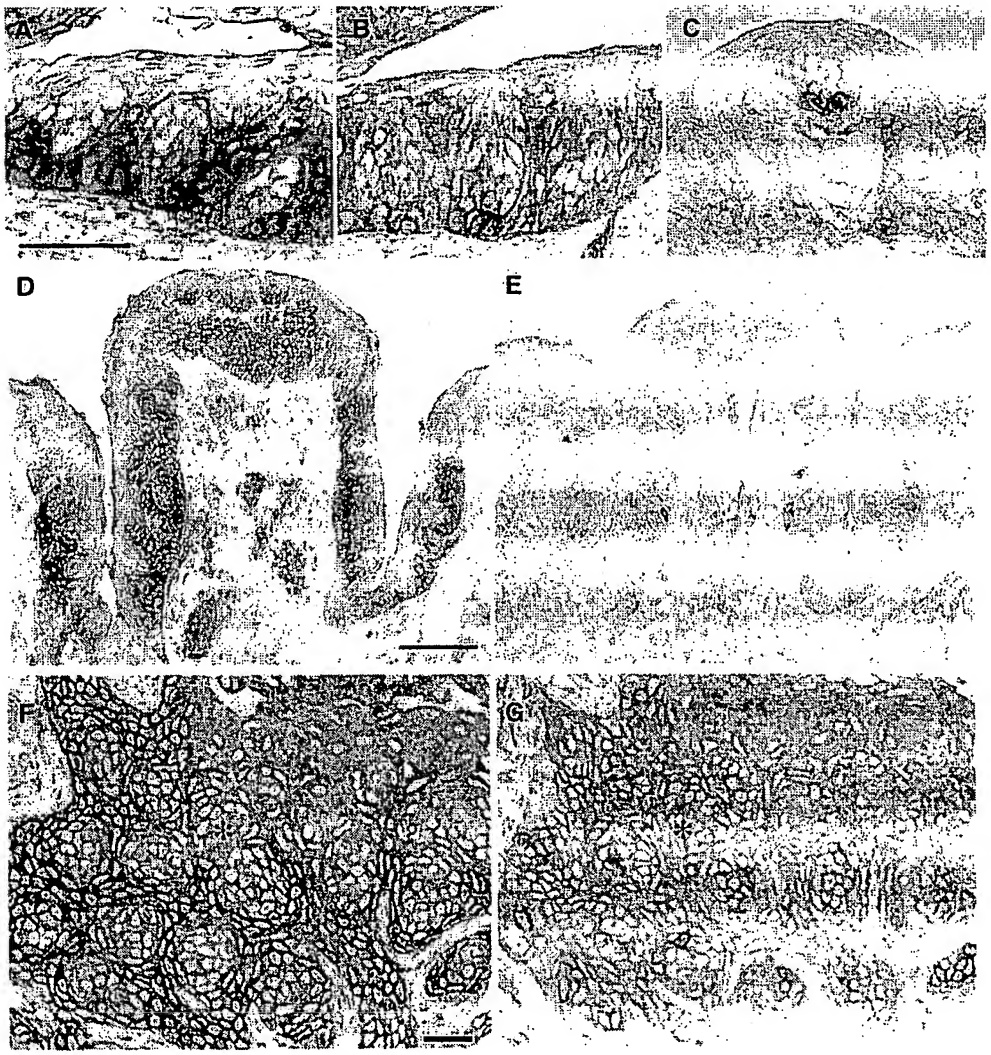

Fig. 1. Expression of *Shh* and *Ptc* in taste papillae of adult mice. Taste buds of circumvallate papillae were analyzed by *Ptc* (A,D,F) and *Shh* (B,E,G). (A) *Ptc* was expressed in epithelial cells adjacent to each taste bud. (B) *Shh* was expressed in basal cells in taste buds. (C) In fungiform papillae, the same expression pattern of *Shh* was observed. Expressions of *Ptc* (D) and *Shh* (E) were restricted to the epithelium containing taste buds but not detectable in the other epithelial region or underlying mesenchyme. The epithelial region of circumvallate papillae was analyzed by *Ptc* (F) and *Shh* (G) in serial adjacent sections. Round-shaped boundaries of each taste bud profile can be identified. (F) In transverse sections of each taste bud, *Ptc* was detected in the basal (white asterisk) but not in the apical (red asterisk) epithelial region surrounding the taste bud. (G) *Shh* was expressed within the taste buds. Clusters of *Shh*-expressing cells were observed in taste buds near the basement membrane (white arrow). Tissues were sectioned at 5 μm, and in situ hybridization was performed as previously described (Asano-Miyoshi et al., 1998). Scale bars, 50 μm (in A) for (A–C); 100 μm (in D) for (D,E); 50 μm (in F) for (F,G).

shown). These observations indicate that the *Shh* and *Ptc* expression is nerve dependent, and those expression disappeared after the denervation of taste buds during the phase in which the taste bud structure was still intact.

Our results show that *Shh* and *Ptc* are associated with the taste bud maintenance by nerve in adult mouse.

2. Methods

The animals used in these experiments as adults were 8–20-week-old C57BL/6N mice. The glossopharyngeal (IXth) nerve crushes was basically performed as described previously (Smith et al., 1994). Adult mice were injected (50 mg/kg i.p.) with bromodeoxyuridine (BrdU) (Roche Molecular Biochemichals) as described previously (Cho et al., 1998). Incorporated BrdU were detected with BrdU Labeling and Detection Kit II (Roche Molecular Biochemichals).

Acknowledgements

This work was supported by BRAIN. The authors thank Dr Kunio Kitamura for the *Shh* cDNA.

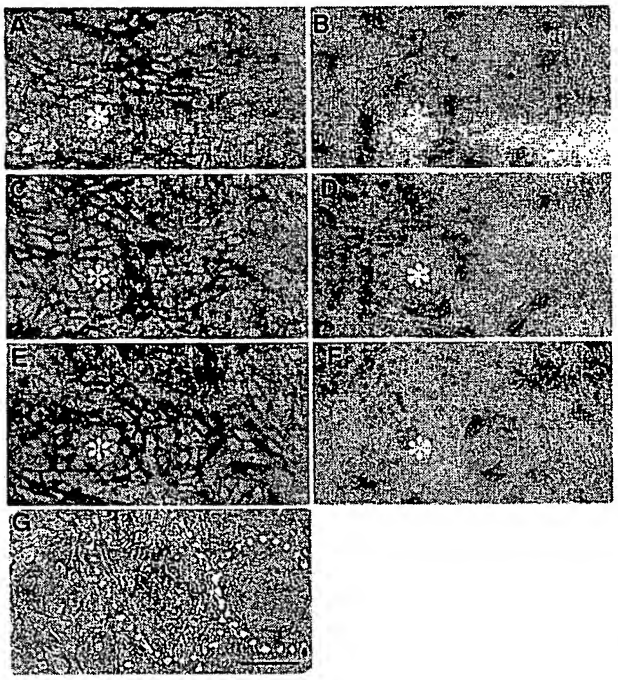

Fig. 2. Comparison between *Ptc* expression and cell proliferation around taste buds in circumvallate papillae of an adult mouse in sagittal sections. (A–F) Serial adjacent sections form apical (A) to basal (F) epithelial regions at 24 h after BrdU injection. (A,C,E) *Ptc* expression was observed around taste buds. (B,D,F) The distribution of BrdU-positive cells corresponded with that of *Ptc* expression. (A–F) Asterisks show an identical taste bud. (D) The taste bud marked with the asterisk exhibits a high-level BrdU uptake in the *Ptc*-expressing region between (C,E), in comparison with (B). (G) At 5.5 days after BrdU injection, BrdU-positive cells were evident within taste buds. Doted lines show outlines of taste buds. Scale bar, 50 μm (in G) for (A–G).

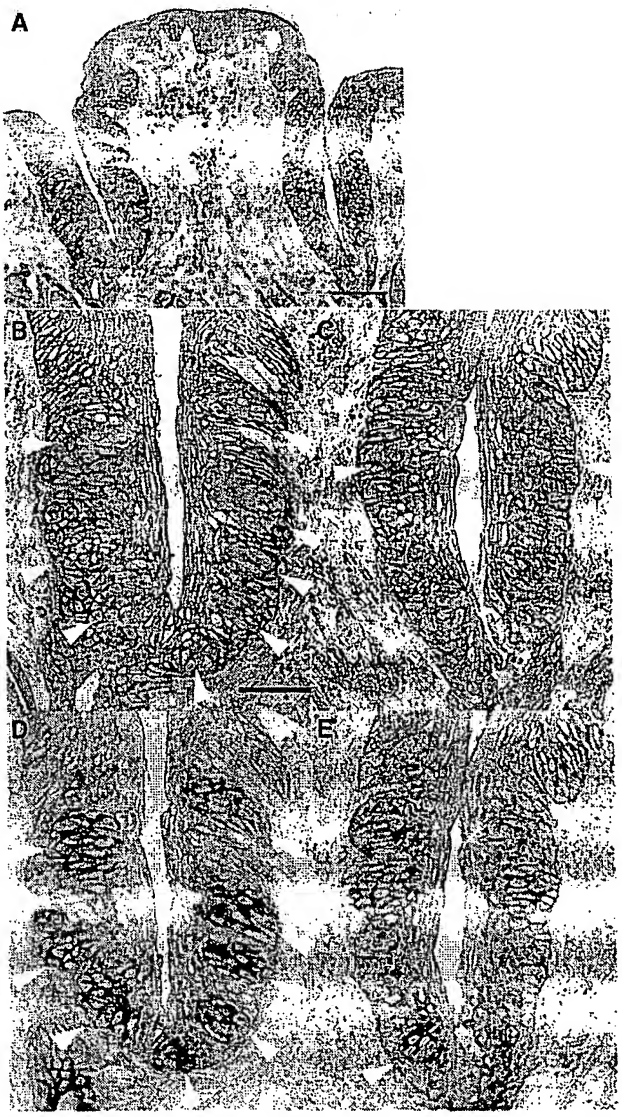

Fig. 3. The disappearance of *Ptc* expression in circumvallate papillae after a right IXth nerve crush. (A) The *Ptc* expression of circumvallate papillae at 4 days after the operation. High-power photomicrograph showing *Ptc* expression in the left (B) and right (C) trench of the circumvallate papillae. (C) *Ptc* expression has almost disappeared in the right trench. The expression of *Keratin8* was analyzed in serial adjacent sections (D, left trench; E, right trench). (E) Expression of *Keratin8* in the right trench indicates the remaining taste bud structure without *Ptc* expression. In the left trench, the taste buds that were indicated by *Keratin8* (D) were surrounded by *Ptc* (B) expression. Arrowheads indicate the taste buds. Scale bars, 100 μm (in A); 50 μm (in B) for (B–E).

References

Asano-Miyoshi, M., Kusakabe, Y., Abe, K., Emori, Y., 1998. Identification of taste-tissue-specific cDNA clones from a subtraction cDNA library of rat circumvallate and foliate papillae. J. Biochem. 124, 927–933.

Beidler, L.M., Smallman, R.L., 1965. Renewal of cells within taste buds. J. Cell Biol. 27, 263–272.

Cho, Y.K., Farbman, A.I., Smith, D.V., 1998. The timing of alpha-gustducin expression during cell renewal in rat vallate taste buds. Chem. Senses 23, 735–742.

Delay, R.J., Kinnamon, J.C., Roper, S.D., 1986. Ultrastructure of mouse vallate taste buds: II. Cell types and cell lineage. J. Comp. Neurol. 253, 242–252.

Farbman, A.I., 1980. Renewal of taste bud cells in rat circumvallate papillae. Cell Tis. Kine. 13, 349–357.

Goodrich, L.V., Johnson, R.L., Milenkovic, L., McMahon, J.A., Scott, M.P., 1996. Conservation of the hedgehog/patched signaling pathway from flies to mice – induction of a mouse patched gene by hedgehog. Genes Dev. 10, 301–312.

Hall, J.M., Hooper, J.E., Finger, T.E., 1999. Expression of sonic hedgehog, patched, and Gli1 in developing taste papillae of the mouse. J. Comp. Neurol. 406, 143–155.

Jung, H-S., Oropeza, V., Thesleff, I., 1999. Shh, Bmp-2, Bmp-4 and Fgf-8 are associated with initiation and patterning of mouse tongue papillae. Mech. Dev. 81, 179–182.

Marigo, V., Scott, M.P., Johnson, R.L., Goodrich, L.V., Tabin, C.J., 1996. Conservation in hedgehog signaling: induction of a chicken patched homolog by Sonic hedgehog in the developing limb. Development 122, 1225–1233.

Smith, D.V., Klevitsky, R., Akeson, R.A., Shipley, M.T., 1994. Expression of the neural cell adhesion molecule (NCAM) and polysialic acid during taste bud degeneration and regeneration. J. Comp. Neurol. 347, 187–196.

Zhang, C., Brandemihl, A., Lau, D., Lawton, A., Oakley, B., 1997. BDNF is required for the normal development of taste neurons in vivo. NeuroReport 8, 1013–1017.